ELSEVIER

Available online at www.sciencedirect.com
SCIENCE DIRECT®

Journal of Chromatography A, 1067 (2005) 145–152

JOURNAL OF CHROMATOGRAPHY A

www.elsevier.com/locate/chroma

Isotope tag method for quantitative analysis of carbohydrates by liquid chromatography–mass spectrometry

Jin Yuan[1], Noritaka Hashii, Nana Kawasaki*, Satsuki Itoh, Toru Kawanishi, Takao Hayakawa

Division of Biological Chemistry and Biologicals, National Institute of Health Sciences, 1-18-1 Kamiyoga, Setagaya-ku, Tokyo 158-8501, Japan

Available online 15 December 2004

Abstract

We have previously demonstrated that liquid chromatography/mass spectrometry equipped with a graphitized carbon column (GCC-LC/MS) is useful for the structural analysis of carbohydrates in a glycoprotein. Here, we studied the monosaccharide composition analysis and quantitative oligosaccharide profiling by GCC-LC/MS. Monosaccharides were labeled with 2-aminopyridine and then separated and monitored by GCC-LC/MS in the selective ion mode. The use of tetradeuterium-labeled pyridylamino (d_4-PA) monosaccharides as internal standards, which were prepared by the tagging of standard monosaccharides with hexadeuterium-labeled 2-aminopyridine (d_6-AP), afforded a good linearity and reproducibility in ESIMS analysis. This method was successfully applied to the monosaccharide composition analysis of model glycoproteins, fetuin, and erythropoietin. For quantitative oligosaccharide profiling, oligosaccharides released from an analyte and a standard glycoprotein were tagged with d_0- and d_6-AP, respectively, and an equal amount of d_0- and d_4-PA oligosaccharides were coinjected into GCC-LC/MS. In this procedure, the oligosaccharides that existed in either analyte or a standard glycoprotein appeared as single ions, and the oligosaccharides that existed in both analyte and a standard glycoprotein were detected as paired ions. The relative amount of analyte oligosaccharides could be determined on the basis of the analyte/internal standard ion-pair intensity ratio. The quantitative oligosaccharide profiling enabled us to make a quantitative and qualitative comparison of glycosylation between the analyte and standard glycoproteins. The isotope tag method can be applicable for quality control and comparability assessment of glycoprotein products as well as the analysis of glycan alteration in some diseases.
© 2004 Elsevier B.V. All rights reserved.

Keywords: Monosaccharides; Oligosaccharides; Pyridylamination; Isotope tag

1. Introduction

A variety of recombinant glycoproteins and modified glycoproteins are developed as medical agents, and most of them exist in heterogeneous forms because of the various combinations of oligosaccharides. Alteration of glycosylation is known to affect the biological activity, mobilization, and biophysical properties of glycoproteins [1], so assessments of their carbohydrate structure and heterogeneity are essential in many stages of development and quality control of glycoprotein products. Since glycosylation varies in response to changes in the manufacturing condition, monosaccharide composition analysis and/or oligosaccharide profiling are needed for the characterization and as a test for constancy and comparability assessments of glycosylation [2]. Several analytical procedures using HPLC have been reported for oligosaccharide profiling and structural analysis of carbohydrates [3–5]. The oligosaccharide profiling using liquid chromatography/mass spectrometry (LC/MS) is especially known to provide structural information from their chromatographic behavior and molecular mass [6–8]. We have developed mass spectrometric oligosaccharide profiling using a graphitized carbon column (GCC), which can separate

Abbreviations: AP, 2-aminopyridine; d_0, non-deuterium-labeled; d_4, tetradeuterium-labeled; d_6, hexadeuterium-labeled; Fuc, fucose; Gal, galactose; GalN, galactosamine; GalNAc, *N*-acetylgalactosamine; GCC, graphitized carbon column; Glc, glucose; GlcN, glucosamine; GlcNAc, *N*-acetylglucosamine; Man, mannose; PA, pyridylamino; R.S.D., relative standard deviation; SIM, selected ion mode; TFA, trifluoroacetic acid; TIC, total ion chromatogram

* Corresponding author. Tel.: +81 3 3700 1141; fax: +81 3 3707 6950.
E-mail address: nana@nihs.go.jp (N. Kawasaki).
[1] Present address: Chendu Institute of Biological Products, 610063, Chengdu Wai Dong Bao Jiang Qiao, Sichuan Province, China.

0021-9673/$ – see front matter © 2004 Elsevier B.V. All rights reserved.
doi:10.1016/j.chroma.2004.11.070

oligosaccharides based on subtle differences in branch, position, and linkage with volatile solution [9,10]. This method enables us to distinguish the glycosylation among some glycoprotein products produced in different cells [11].

A use of internal standards is known to improve the precision and linearity in quantitative analyses. Isotopic analogs of the analytes are currently the preferred internal standards for quantification by mass spectrometry (MS) procedures. For instance, Gygi et al. [12] demonstrated the approach for the accurate quantification of the proteins within complex mixture using isotope-coded affinity tags (ICATs). The use of the isotope-labeled carbohydrates as internal standards can make it possible to quantify the carbohydrates by LC/MS. Reductive pyridylamination is frequently used for the tagging of carbohydrates in HPLC analysis [13,14]. This derivatization is known to afford higher sensitivity in MS analysis [15], and PA oligosaccharides were reported to be separated by GCC [16]. Here, we study quantitative analysis of carbohydrates using tetradeuterium-labeled pyridylamino (d_4-PA) carbohydrates as internal standards. First, we study the monosaccharide composition analysis by using d_4-PA monosaccharides as internal standards. Next, the isotope tag method is used for the quantitative oligosaccharide profiling using recombinant human chorionic gonadotropin (rhCG) and human chorionic gonadotropin (hCG) as an analyte and standard glycoproteins, respectively.

2. Materials and methods

2.1. Materials

All monosaccharide standards were purchased from Seikagaku-kogyo (Tokyo, Japan). The pyridylamination apparatus (PALSTATION), reagents for the pyridylamination reaction, and PA monosaccharide standards were available from TaKaRa Biomedicals (Otsu, Japan). The hexadeuterium-labeled 2-aminopyridine (d_6-AP) was purchased from Wako (Osaka, Japan). Human chorionic gonadotropin (hCG) and recombinant hCG (rhCG) were bought from Sigma (St. Louis, MO, USA). *N*-glycosidase F was purchased from Roche Diagnostics. All other chemicals and reagents were of analytical grade and were commercially available.

2.2. Pyridylamination of monosaccharides

For the pyridylamination of amino sugars, free amino groups of monosaccharides (GlcN, GalN, 1–1000 pmol) were acetylated by incubation in 50 μl of methanol/pyridine/distilled water (30/15/10, v/v/v) with 2 μl of acetic anhydride for 30 min at room temperature. The mixture was dried using a vacuum centrifuge evaporator without heating. Acetic acid (50 μl), methanol (60 μl), and 10 μl of coupling reagent prepared by mixing 100 mg of AP was added to monosaccharides (Fuc, Gal, Glc, Man, GlcNAc, GalNAc, 1–1000 pmol). The mixture was heated at 90 °C for 20 min by PALSTATION, and the excess reagents were removed by evaporation under a stream of nitrogen gas at 60 °C for 20 min. Then 10 μl of a reducing reagent, prepared just before use by mixing 6 mg of borane–dimethylamine complex and 100 μl of acetic acid, was added, and the mixture was heated at 90 °C for 35 min. The reaction mixture was dried three times under a stream of nitrogen gas at 50 °C for 10 min. The residue was dissolved in water for LC/MS analysis. For the preparation of isotope analogs, the tetradeuterium-labeled PA (d_4-PA) monosaccharide, d_0-AP was just replaced by d_6-AP (Fig. 1).

2.3. Monosaccharide composition analysis of a glycoprotein

A glycoprotein (25 pmol) was placed in a hydrolysis tube fitted with a Teflon-lined screw cap. Fifty microliters of 2 M HCl-2M trifluoroacetic acid (TFA) was added to the sample, which was then heated at 100 °C for 6 h. Simultaneously, a set of monosaccharide standards, 100 pmol of Gal, Man, Glc, Fuc, GlcN, and GalN, was treated identically as the analytes. The solution obtained was freeze-dried. The monosaccharides obtained from the analyte glycoproteins and standard monosaccharides were tagged with non-deuterium-labeled 2-aminopyridine (d_0-AP) and d_6-AP, respectively. Each tagged oligosaccharide mixture was dissolved into purified water, and a mixture of d_0- and d_4-PA monosaccharides was injected into the GCC-LC/MS.

2.4. Preparation of N-linked oligosaccharides

N-linked oligosaccharides were released from hCG as described previously [17]. Briefly, hCG and rhCG (100 μg)

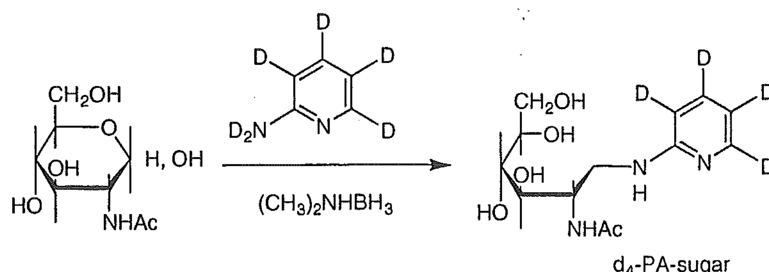

Fig. 1. Synthesis of d_4-PA monosaccharide internal standard.

were dissolved in 360 μl of 0.5 M Tris–HCl buffer (pH 8.6), containing 8 M guanidine hydrochloride and 5 mM ethylenediaminetetra-acetic acid (EDTA). After an addition of 2.6 μl of 2-mercaptethanol, the mixture was allowed to stand at room temperature for 2 h. To this solution, 7.56 mg of monoiodoacetic acid was added, and the resulting mixture was incubated at room temperature for 2 h in the dark. The reaction mixture was applied to a PD-10 column (Amershambioscience, Uppsala, Sweden) to remove the reagents, and the eluate was lyophilized.

Carboxymethylated hCG and rhCG were dissolved in 100 μl of 0.1 M sodium phosphate buffer, pH 7.2, and incubated with 5 units of PNGase F at 37 °C for 2 days. Protein was precipitated with 340 μl of cold ethanol, and the supernatant was dried.

2.5. Pyridylamination of oligosaccharides from hCG

To the lyophilized oligosaccharides released from rhCG we added 10 μl of coupling reagent prepared by mixing 300 mg of d_0-AP, and 100 μl of acetic acid, and the reaction mixture was heated at 90 °C for 60 min. Then, 10 μl of a reducing reagent, prepared just before use by mixing 20 mg of borane–dimethylamine complex and 100 μl of acetic acid, was added, and the mixture was heated at 80 °C for 60 min. The reaction mixture was dried three times under a stream of nitrogen gas at 60 °C for 10 min. The residue was dissolved in water for LC/MS analysis. For the preparation of the tetradeuterium-labeled (d_4)-PA oligosaccharide isotope analogs, d_0-AP was just replaced by d_6-2-aminopyridine.

2.6. LC/MS analysis

LC was carried out using a Magic 2002 HPLC system (Michrom BioResources Inc., Auburn, CA, USA) using a Hypercarb column (0.2 mm × 150 mm, Thermoelectron, San Jose, CA, USA). The flow rate was set at 2–3 μl/min through a splitter system. The mobile phases were 5 mM ammonium acetate (pH 8.5) with 2% of acetonitrile (pump A) and 80% of acetonitrile (pump B). A gradient of 10–35% of B in 60 min was used for the monosaccharide analysis. For oligosaccharide profiling, we used a gradient of 5–20% of B in 20 min, 20–70% of B in 15 min, and 70–95% of B in 5 min. The mass spectrometer used was a TSQ 7000 (Thermoelectron) equipped with a nanoelectrospray ion source (AMR Inc., Tokyo, Japan). The ESI voltage was set to 2000 V (positive ion mode) or 1500 V (negative ion mode), and the capillary temperature was 175 °C.

3. Results

3.1. Monosaccharide composition analysis using the isotope tag method

First, we examined the possibility of the isotope-tag method for the monosaccharide composition analysis of gly-

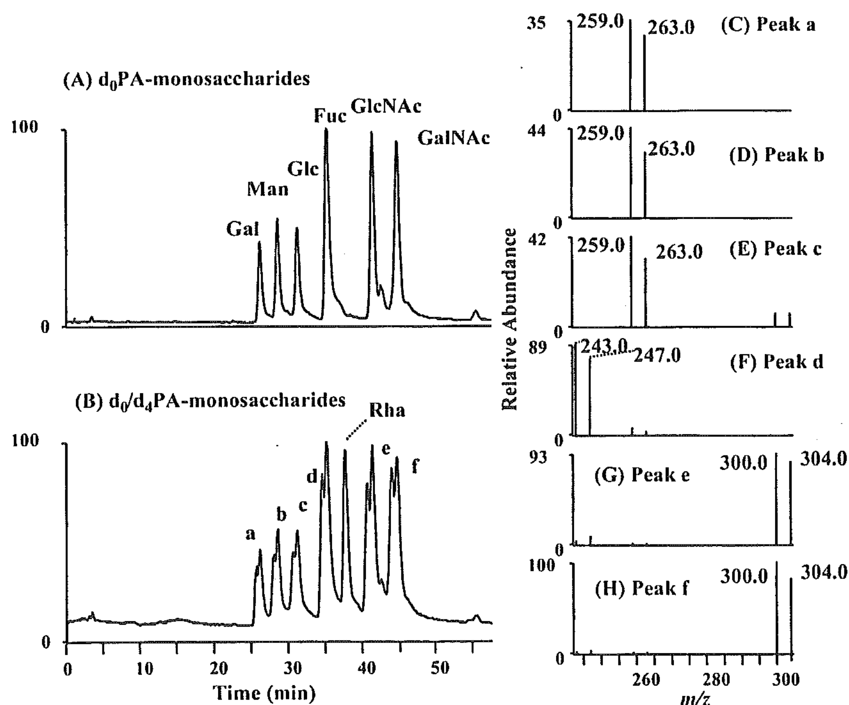

Fig. 2. (A) Extracted ion chromatogram (set m/z values, 243, 259, and 300) of d_0-PA monosaccharides (1 pmol Gal, Man, Glc, Fuc, GlcNAc, and GalNAc). (B) Extracted ion chromatogram (set m/z values, 243, 247, 259, 263, 300, and 304) of a mixture of d_0- and d_4-PA monosaccharides (1 pmol Gal, Man, Glc, Fuc, Rham, GlcNAc and GalNAc). (C) Mass spectra of peaks a (C), b (D), c (E), d (F), e (G), and f (H).

coproteins. An equal molar of each d_0-PA monosaccharide (Gal, Man, Glc, Fuc, GlcNAc, and GalNAc, 1 pmol each) was analyzed by GCC-LC/MS in the positive ion mode. The ions monitored were *m/z* 259 (for d_0-PA-Gal, d_0-PA-Man, and d_0-PA-Glc), *m/z* 243 (d_0-PA-Fuc), and *m/z* 300 (d_0-PA-GlcNAc and d_0-PA-GalNAc). Fig. 2A shows the mass chromatogram of the d_0-PA monosaccharides. All six d_0-PA monosaccharides were retained and separated by GCC. The detection limit at a signal-to-noise ratio of 3 was 45 fmol.

The d_4-PA monosaccharides were prepared as internal standards by tagging of standard monosaccharides with d_6-AP and combined with d_0-PA monosaccharides. Fig. 2B shows the chromatogram of a mixture of d_0-, d_4-PA monosaccharides and PA-labeled Rhamnose, which is frequently used as an internal standard in the monosaccharide composition analysis. Paired ions with a difference of *m/z* 4 were detected in the mass spectra of peaks a–f (Fig. 2C–H). When 0.5 pmol d_0-PA monosaccharides were determined in the presence of d_4-PA monosaccharides or Rhamnose by GCC-LC/MS, the relative standard deviation ($n = 5$) was 1.8–4.8% or 5.6–8.3%, respectively.

To assess the linearity and reproducibility of the whole procedure, including reacetylation, pyridylamination, the removal of excess derivatization reagents, and GCC-LC/MS, we tagged different amounts of monosaccharides (Gal, Man, Glc, Fuc, GlcN, and GalN, 1–1000 pmol) with d_0-AP, and d_4-PA monosaccharides (4 or 20 pmol) were added to the d_0-PA monosaccharides (1–10 pmol or 10–1000 pmol, respectively). The whole process of the isotope tag method was found to be linear for all six monosaccharides over the tested range of 1–1000 pmol (Fig. 3). The accuracy of this method was approximately 80–100% (Fig. 3), and the relative standard deviations (%R.S.D.) were less than 7.2% for all monosaccharides (based on the peak area ratio of monosaccharides from five samples).

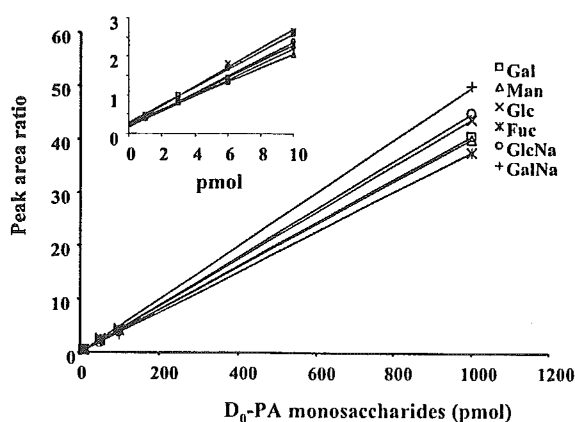

Fig. 3. Linearity on the isotope-tag method for monosaccharide quantification. For the internal standards, 1000 pmol monosaccharides were derivatized to d_4-PA monosaccharides. Different amounts of monosaccharides were derivatized to d_0-PA monosaccharides and co-injected with 4 pmol (A) or 20 pmol (B) internal standards into GCC-LC/MS.

We used this method for the monosaccharide composition analysis of fetuin and erythropoietin. Accuracy in the monosaccharide composition analysis of a glycoprotein relies on the condition of hydrolysis. Fan et al. [18] studied the hydrolysis of N-linked oligosaccharides and recommended 4 h with 2 M TFA at 100 °C for neutral sugars, and 6 h with 4 M HCl at 100 °C for amino sugars. While these hydrolysis conditions result in the complete release of neutral and amino sugars with no degradation, it takes two hydrolyses for a single sample. To quantify both neutral and amino sugars in glycoproteins in the same run, fetuin and erythropoietin (25 pmol) were heated in 2 M HCl-2M TFA at 100 °C for 6 h [19], and a set of monosaccharide standards, 100 pmol of Gal, Man, Glc, Fuc, GlcN, and GalN, was treated identically as the analyte glycoproteins. After hydrolysis, the analyte and standard monosaccharides were tagged with d_0- and d_6-AP, respectively. Fig. 4A and E show the mass chromatogram of monosaccharides prepared from fetuin and erythropoietin in the presence of d_4-PA monosaccharides, respectively.

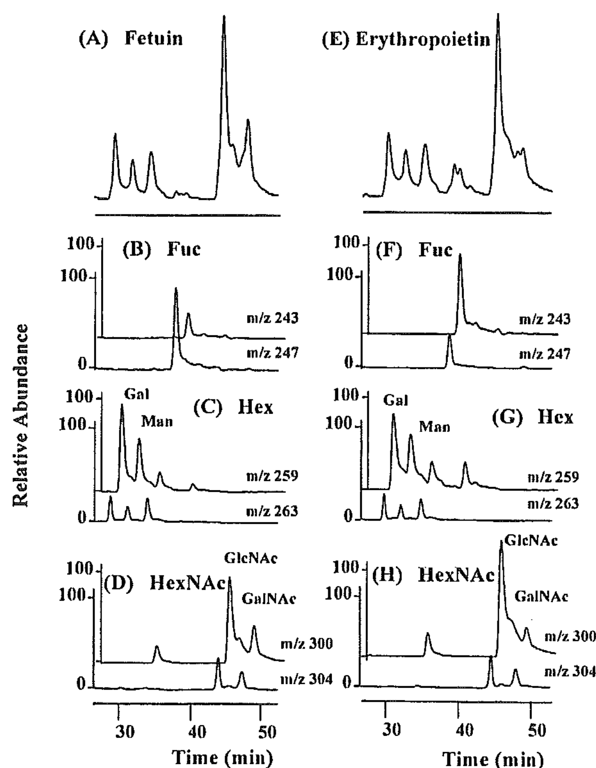

Fig. 4. Monosaccharide composition analysis of glycoproteins. Extracted ion chromatograms of d_0-PA monosaccharides from fetuin and d_4-PA standard monosaccharides (set *m/z* values, 243, 247, 259, 263, 300, and 304) (A), d_0-PA Fuc from fetuin and d_4-PA standard Fuc (set *m/z* values, 243 and 247) (B), d_0-PA Hex from fetuin and d_4-PA standard Hex (set *m/z* values, 259 and 263) (C), and d_0-PA HexNAc from fetuin and d_4-PA standard HexNAc and (set *m/z* values, 300 and 304) (D). Extracted ion chromatograms of d_0-PA monosaccharides from erythropoietin and d_4-PA standard monosaccharides and (set *m/z* values, 243, 247, 259, 263, 300, and 304) (E), d_0-PA Fuc from erythropoietin and d_4-PA standard Fuc (set *m/z* values, 243 and 247) (F), d_0-PA Hex from erythropoietin and d_4-PA standard Hex (set *m/z* values, 259 and 263) (G), and d_0-PA HexNAc from erythropoietin and d_4-PA standard HexNAc (set *m/z* values, 300 and 304) (H).

Table 1
Monosaccharide composition analysis by isotope-tag method

Glycoprotein	Monosaccharide	mol/mol[a]	mol/mol
Fetuin	Fuc	0.3	0 [20]
	Gal	10.4	12
	Man	7.6	9
	GlcNAc	14.7	15
	GalNAc	3.4	3
Erythropoietin	Fuc	3.4	4.1 [21]
	Gal	12.8	13.8
	Man	8.1	8.7
	GlcNAc	15.6	17.2
	GalNAc	1.5	0.9

[a] Values were expressed as mol detected in 1 mol glycoprotein.

Fig. 4B, and F show the mass chromatograms of d_0-, and d_4-PA fucose, Fig. 4C and G indicate those of d_0-, d_4-PA hexose, and Fig. 4D and H show those of d_0-, d_4-PA HexNAc. The monosaccharide compositions of fetuin and erythropoietin calculated from the peak area ratios (d_0-PA/d_4-PA monosaccharides) were in good agreement with the reported values (Table 1) [20,21]. By heating the standard monosaccharides simultaneously the decomposition of monosacchrides during hydrolysis can be corrected, and a use of isotope analogs as the internal standards can reduce deviation in ESIMS analysis.

3.2. Quantitative oligosaccharide profiling using the isotope tag method

Next, we explored the capability of the isotope-tag method for the quantitative oligosaccharide profiling. When d_0-PA oligosaccharides prepared from an analyte glycoprotein are analyzed with an equal part of d_4-PA oligosaccharides prepared from a standard glycoprotein, oligosaccharides which link to both the analyte and the standard glycoproteins are expected to appear as paired ions with a difference of 4 Da, and the individual oligosaccharides in the analyte glycoprotein can be quantified based on the analyte/internal standard ion-pair intensity ratio. On the other hand, any oligosaccharides that link to either the analyte or the standard glycoprotein ought to be detected as single ions. Oligosaccharides released from rhCG and hCG were tagged with d_0- and d_6-AP, respectively, and the tagged oligosaccharides were analyzed by GCC-LC/MS in both positive and negative ion modes.

Fig. 5A and B show the mass spectra of the peak which was detected at 21.5 min in the positive and the negative ion mode, respectively. In the positive ion mode, ions at *m/z* 863.0, 1359.4 and 1197.2 were detected (Fig. 5A), and they can be assigned to d_4-PA $[Hex]_5[HexNAc]_4^{2+}$ (an asialobiantennary oligosaccharide), d_4-PA$[Hex]_3[HexNAc]_4^{+}$ (a fragment of the asialobiantennary form) and d_4-PA$[Hex]_4[HexNAc]_4^{+}$ (a fragment of the asialobiantennary form), respectively. In contrast, only an ion at *m/z* 860.9 (d_4-PA$[Hex]_5[HexNAc]_4^{2-}$, asialobiantennary oligosaccharide) was detected in the negative ion mode (Fig. 5B). This result suggests that mass spectra

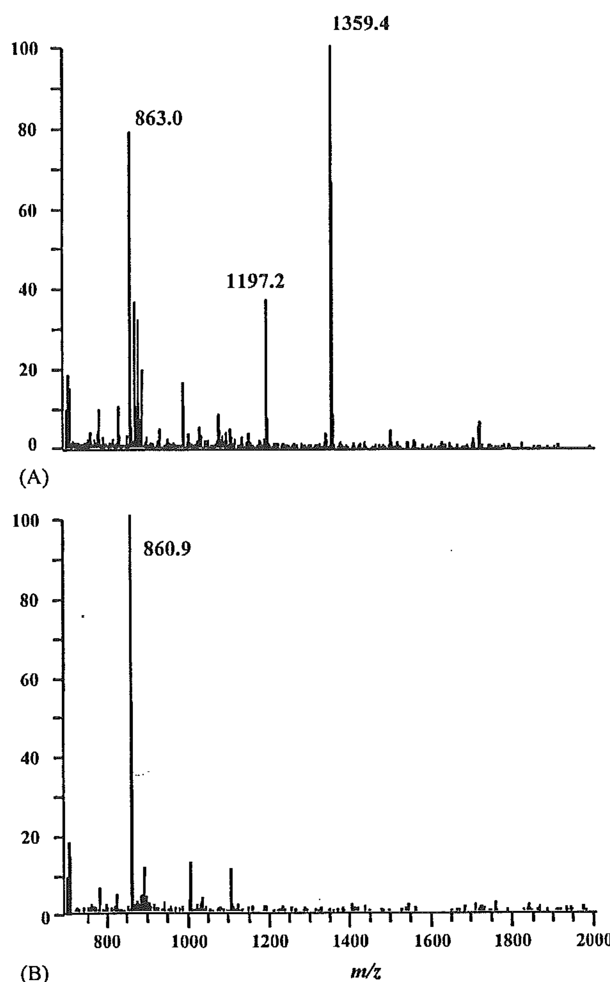

Fig. 5. Mass spectra of d_4-PA oligosaccharide. D_4-PA oligosaccharide eluted at 21.5 min from GCC was analyzed by ESIMS in the positive ion mode (A) and negative ion mode (B).

of PA oligosaccharides become complicated due to fragmentation in the positive ion mode, while only molecular ions can be detected in the negative ion mode. Therefore, ESI analysis in the negative ion mode was chosen for the PA oligosaccharide profiling.

Fig. 6A and B show the TIC of a mixture of equal parts of d_0-PA oligosaccharides prepared from rhCG and d_4-PA oligosaccharides from hCG, and its two-dimensional display (retention time versus *m/z*), respectively. The carbohydrate structures, which can be deduced from *m/z* values, are indicated in Table 2. Paired ions at *m/z* 757.5, 759.5 were observed in the mass spectrum of peak a1. Based on carbohydrate composition $[Hex]_5[HexNAc]_3$, it can be assigned to a hybrid type oligosaccharide. Likewise, peak 11, 12, 14, 15, p1, p2, and p4 consisted of paired ions and can be assigned to monosialylated (11, 12, 14, 15) and disialylated (p1, p2) biantennary oligosaccharide without Fuc. Fig. 7 shows TIC of d_0-, d_4-PA oligosaccharides (A), extracted ion chromatograms of d_0-PA (B), d_4-PA (C), and d_0-, d_4-PA monosialylated biantennary form (D). The mass spectra of peaks 11–15 are shown in Fig. 7E–I. Peak 13 was not observed in Fig. 7D and only

Table 2
Structural assignment of peaks in Fig. 6B

Peak nos.	Carbohydrate composition[a]	Deduced structure[b]	Theoretical mass (d_0-PA-sugar)	Observed m/z			Ion-pair intensity ratio d_0/d_4
				d_0-PA-rhCG	d_4-PA-hCG		
				M^{2-}	M^{3-}	M^{2-}	
a1	[Hex]$_5$[HexNAc]$_3$	Hybrid (1)	1517.5	757.5		759.5	0.27
b1	[Hex]$_5$[HexNAc]$_4$[NeuNAc]$_2$	Bi + NA$_2$	2303.1		768.2		
c1	[Fuc]$_1$[Hex]$_5$[HexNAc]$_4$[NeuNAc]$_2$	FBi + NA$_2$	2449.3		816.7		
d1	[Hex]$_4$[HexNAc]$_3$[NeuNAc]$_1$	Mono + NA	1646.6			824.3	
d2	[Hex]$_4$[HexNAc]$_3$[NeuNAc]$_1$	Mono + NA	1646.6			824.0	
e1	[Hex]$_6$[HexNAc]$_3$	Hybrid (2)	1679.6	838.6			
e2	[Hex]$_6$[HexNAc]$_3$	Hybrid (2)	1679.6			840.6	
f1	[Hex]$_5$[HexNAc]$_4$	Bi	1720.7	858.9			
f2	[Hex]$_5$[HexNAc]$_4$	Bi	1720.7			861.2	
g1	[Hex]$_5$[HexNAc]$_3$[NeuNAc]$_1$	Hybrid (1) + NA	1807.7	902.9			
g2	[Hex]$_5$[HexNAc]$_3$[NeuNAc]$_1$	Hybrid (1) + NA	1808.7			905.0	
h1	[Fuc]$_1$[Hex]$_5$[HexNAc]$_4$	FBi	1866.8			934.0	
i1	[Hex]$_6$[HexNAc]$_4$	Hybrid (3)	1882.8	940.2			
j1	[Hex]$_5$[HexNAc]$_5$	Bi + GN	1924.9			962.7	
k1	[Hex]$_6$[HexNAc]$_3$[NeuNAc]$_1$	Hybrid (2) + NA	1970.8			986.8	
k2	[Hex]$_6$[HexNAc]$_3$[NeuNAc]$_1$	Hybrid (2) + NA	1970.8			986.2	
l1	[Hex]$_5$[HexNAc]$_4$[NeuNAc]$_1$	Bi + NA	2011.9	1004.7		1006.7	0.77
l2	[Hex]$_5$[HexNAc]$_4$[NeuNAc]$_1$	Bi + NA	2011.9	1004.6		1007.3	0.56
l3	[Hex]$_5$[HexNAc]$_4$[NeuNAc]$_1$	Bi + NA	2011.9	1004.6			
l4	[Hex]$_5$[HexNAc]$_4$[NeuNAc]$_1$	Bi + NA	2011.9	1004.6		1006.5	0.67
l5	[Hex]$_5$[HexNAc]$_4$[NeuNAc]$_1$	Bi + NA	2011.9	1004.6		1006.4	0.49
m1	[Hex]$_7$[HexNAc]$_4$	Hybrid (4)	2044.9	1021.4			
n1	[Fuc]$_1$[Hex]$_5$[HexNAc]$_4$[NeuNAc]$_1$	FBi + NA	2158.0			1079.8	
n2	[Fuc]$_1$[Hex]$_5$[HexNAc]$_4$[NeuNAc]$_1$	FBi + NA	2158.0			1079.8	
n3	[Fuc]$_1$[Hex]$_5$[HexNAc]$_4$[NeuNAc]$_1$	FBi + NA	2158.0			1079.8	
o1	[Hex]$_6$[HexNAc]$_4$[NeuNAc]$_1$	Hybrid (3) + NA	2174.0	1085.6			
o2	[Hex]$_6$[HexNAc]$_4$[NeuNAc]$_1$	Hybrid (3) + NA	2174.0	1085.7			
p1	[Hex]$_5$[HexNAc]$_4$[NeuNAc]$_2$	Bi + NA$_2$	2303.1	1150.3		1152.1	5.76
p2	[Hex]$_5$[HexNAc]$_4$[NeuNAc]$_2$	Bi + NA$_2$	2303.1	1150.2		1152.2	5.92
p3	[Hex]$_5$[HexNAc]$_4$[NeuNAc]$_2$	Bi + NA$_2$	2303.1	1150.1			
p4	[Hex]$_5$[HexNAc]$_4$[NeuNAc]$_2$	Bi + NA$_2$	2303.1	1150.3		1152.4	0.45

[a] Hex, hexsose; HexNAc, *N*-acetyl hexsosamine; NeuNAc, *N*-acetyl neuraminic acid; Fuc, fucose.
[b] Abbreviations and structures. The structures are based on the previous reports.

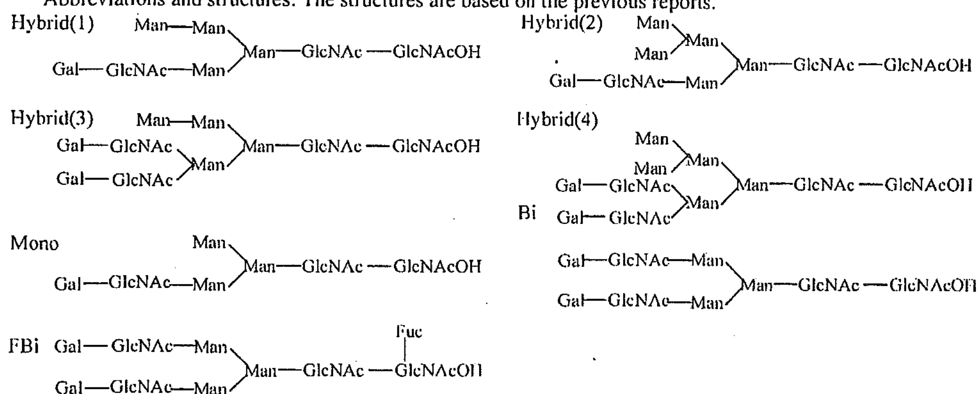

single ion was detected in Fig. 7G. These results suggest that one of monosialylated binantenary oligosaccharides isomers links to only rhCG.

We determined relative amounts of some oligosaccharides in rhCG on the basis of ion-pair intensity ratios (Table 2). The amount of monosialylated biantennary forms (l1, l2, l4, and l5) linked to rhCG were 50–70% of those to hCG. The amount of disialylated biantennary forms (p1 and p2) linked to rhCG was five-fold of those to hCG, and the linkage of p4 to rhCG was one-half of that of hCG. The isotope tag method clearly shows the difference in distribution of isomers between rhCG and hCG.

In this procedure, oligosaccharides linked to either rhCG or hCG were detected as single ions. As shown in Table 2, nine oligosaccharides were detected as single ions in rhCG, and they are reduced to hybrid type and complex type.

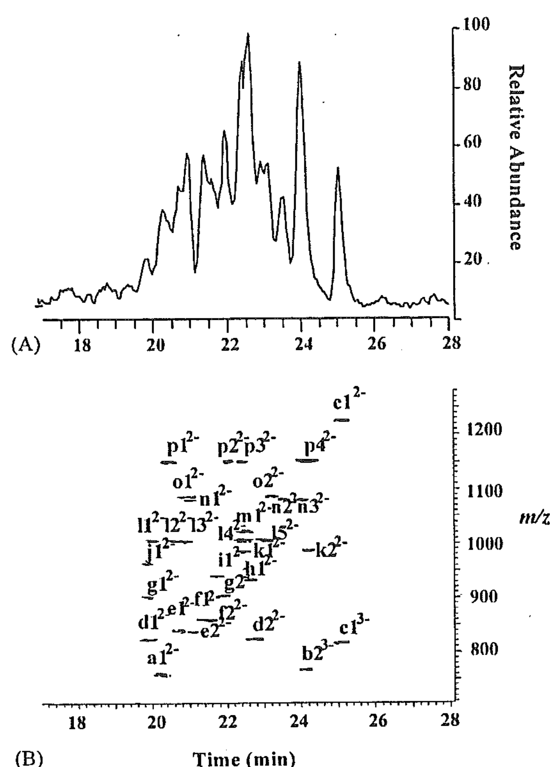

Fig. 6. TIC of a mixture of equal amount of d_0-PA N-linked oligosaccharides from rhCG and d_4-PA N-linked oligosaccharides from hCG (A), and its 2D display (B). Oligosaccharides (from 2 μg rhCG and hCG) were analyzed by GCC-LC/MS in the negative ion mode.

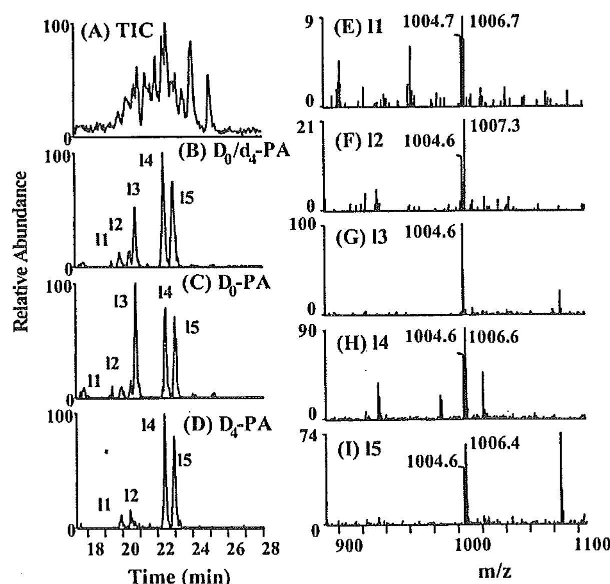

Fig. 7. TIC of a mixture of equal amount of d_0-PA N-linked oligosaccharides from rhCG and d_4-PA N-linked oligosaccharides from hCG (A). Extracted ion chromatograms of d_0-, and d_4-PA monosialylated biantennary (set *m/z* values, 1004–1007) (B), d_0-PA monosialylated biantennary (set *m/z* values, 1004–1005) (C), and d_4-PA monosialylated biantennary oligosaccharides (set *m/z* values, 1006–1007) (D). Mass spectra of peak 11–15 (E–I).

Fourteen oligosaccharides were detected only in hCG, and most of them were fucosylated complex type. These results show the differences in glycosylation between rhCG and hCG and suggest that many hybrid type oligosaccharides linked to rhCG, while fucosylated oligosaccharides attach to hCG.

4. Discussion

Alteration of glycosylation is known to cause many changes in the biological activity as well as the physical properties of proteins. Several procedures of oligosaccharide profiling have been reported for the assessment of alteration of glycosylation, however, most of them can be used for only either qualitative or quantitative analysis. Although mass spectrometric oligosaccharide profiling is useful for the qualitative analysis, it has a problem on precision, and some isomers are still indistinguishable if their retention times are closed to others. In this study, we demonstrated that the use of isotope-tagged internal standards and GCC-LC/MS made it possible to do both quantitative and qualitative carbohydrate analysis.

First, we demonstrated the monosaccharide composition analysis using the isotope tag method. The use of internal standards that were heated under the same hydrolysis condition as an analyte glycoprotein resulted in good precision and accuracy in the monosaccharide composition analysis. Several HPLC methods for determination of monosaccharides have been reported. High-performance anion-exchange chromatography with pulsed amperometric detection (HPAEC-PAD) has been widely used for monosaccharide composition analysis [20,22–25]. Although HPAEC-PAD gives high resolution of all common monosaccharides and has the advantage of not requiring derivatization, this method is also known to have a disadvantage of limited selectivity [26]. The isotope tag method with SIM mode is equal to the HPAEC-PAD in sensitivity and is better than it in selectivity.

Next, we demonstrated the potentiality of the isotope tag method for quantitative oligosaccharide profiling using rhCG and hCG as model glycoproteins. hCG consists of an α subunit (MW 14.7 kDa) and a β subunit (MW 23.0 kDa), and oligosaccharides link to Asn52, and 78 in the α subunit and Asn13 and 30 in the β subunit. It has been reported that the majority of N-linked oligosaccharides in rhCG and hCG are fucosylated or non-fucosylated di-, tri-, and tetra-antennary forms with a various level of sialylation [27–30]. We prepared d_0-PA oligosaccharides and d_4-PA oligosaccharides from rhCG and hCG, respectively, and an equal part of d_0-PA and d_4-PA oligosaccharides was injected into LC/MS. We demonstrated that the oligosaccharides existing in one side protein were detected as single ions, whereas common oligosaccharides were detected as paired ions. We could easily realize that monosialo-, and disialobiantennary oligosaccharides linked to both hCG and rhCG, while fucosylated oligosaccharides and some hybrid type oligosaccharides linked to only hCG and rhCG, respectively. In addition, we demonstrated the pos-

sibility of the quantitative comparison the oligosaccharides between two quite similar glycoproteins. This quantitative oligosaccharide profiling is expected to be a powerful tool in various stages, including quality control and comparability assessment of glycoprotein products, and elucidation of glycan alteration in some diseases.

Acknowledgements

This study was supported in part by the Japan–China Sasakawa Medical Fellowship (J.Y.) and by a grant-in-aid for Research on Health Sciences focusing on Drug Innovation from The Japan Health Sciences Foundation (N.K.).

References

[1] A. Varki, Glycobiology 3 (1993) 97.
[2] T. Hayakawa, in: Y.-y.H. Chiu, J.L. Gueriguian (Eds.), Drug Biotechnology Regulation. Scientific Basis and Practices, Marcel Dekker Inc., New York, 1991, p. 468.
[3] N. Takahashi, H. Nakagawa, K. Fujikawa, Y. Kawamura, N. Tomiya, Anal. Biochem. 226 (1995) 139.
[4] R.R. Townsend, M.R. Hardy, O. Hindsgaul, Y.C. Lee, Anal. Biochem. 174 (1988) 459.
[5] G.R. Guile, P.M. Rudd, D.R. Wing, S.B. Prime, R.A. Dwek, Anal. Biochem. 240 (1996) 210.
[6] L. Royle, T.S. Mattu, E. Hart, J.I. Langridge, A.H. Merry, N. Murphy, D.J. Harvey, R.A. Dwek, P.M. Rudd, Anal. Biochem. 304 (2002) 70.
[7] J. Delaney, P. Vouros, Rapid Commun. Mass Spectrom. 15 (2001) 325.
[8] K.A. Thomsson, H. Karlsson, G.C. Hansson, Anal. Chem. 72 (2000) 4543.
[9] N. Kawasaki, M. Ohta, S. Hyuga, M. Hyuga, T. Hayakawa, Anal. Biochem. 285 (2000) 82.
[10] N. Kawasaki, S. Itoh, M. Ohta, T. Hayakawa, Anal. Biochem. 316 (2003) 15.
[11] N. Kawasaki, M. Ohta, S. Itoh, M. Hyuga, S. Hyuga, T. Hayakawa, Biologicals 30 (2002) 113.
[12] S.P. Gygi, B. Rist, S.A. Gerber, F. Turecek, M.H. Gelb, R. Aebersold, Nat. Biotechnol. 17 (1999) 994.
[13] S. Hase, T. Ikenaka, Y. Matsushima, Biochem. Biophys. Res. Commun. 85 (1978) 257.
[14] S. Hase, S. Hara, Y. Matsushima, J. Biochem. (Tokyo) 85 (1979) 217.
[15] S. Suzuki, K. Kakehi, S. Honda, Anal. Chem. 68 (1996) 2073.
[16] M. Wuhrer, H. Geyer, M. von der Ohe, R. Gerardy-Schahn, M. Schachner, R. Geyer, Biochimie 85 (2003) 207.
[17] S. Itoh, N. Kawasaki, M. Ohta, T. Hayakawa, J. Chromatogr. A 978 (2002) 141.
[18] J.Q. Fan, Y. Namiki, K. Matsuoka, Y.C. Lee, Anal. Biochem. 219 (1994) 375.
[19] H. Takemoto, S. Hase, T. Ikenaka, Anal. Biochem. 145 (1985) 245.
[20] M.R. Hardy, R.R. Townsend, Y.C. Lee, Anal. Biochem. 170 (1988) 54.
[21] H. Sasaki, B. Bothner, A. Dell, M. Fukuda, J. Biol. Chem. 262 (1987) 12059.
[22] M.R. Hardy, Methods Enzymol. 179 (1989) 76.
[23] C.C. Ip, V. Manam, R. Hepler, J.P. Hennessey Jr., Anal. Biochem. 201 (1992) 343.
[24] A. Lampio, J. Finne, Anal. Biochem. 197 (1991) 132.
[25] Y.C. Lee, Anal. Biochem. 189 (1990) 151.
[26] M. Weitzhandler, C. Pohl, J. Rohrer, L. Narayanan, R. Slingsby, N. Avdalovic, Anal. Biochem. 241 (1996) 128.
[27] A. Kobata, J. Cell Biochem. 37 (1988) 79.
[28] Y. Endo, K. Yamashita, Y. Tachibana, S. Tojo, A. Kobata, J. Biochem. (Tokyo) 85 (1979) 669.
[29] A. Amoresano, R. Siciliano, S. Orru, R. Napoleoni, V. Altarocca, E. De Luca, A. Sirna, P. Pucci, Eur. J. Biochem. 242 (1996) 608.
[30] A. Gervais, Y.A. Hammel, S. Pelloux, P. Lepage, G. Baer, N. Carte, O. Sorokine, J.M. Strub, R. Koerner, E. Leize, A. Van Dorsselaer, Glycobiology 13 (2003) 179.

Regular Article

Glycomic/glycoproteomic analysis by liquid chromatography/mass spectrometry: Analysis of glycan structural alteration in cells

Noritaka Hashii, Nana Kawasaki, Satsuki Itoh, Mashashi Hyuga, Toru Kawanishi and Takao Hayakawa

Division of Biological Chemistry and Biologicals, National Institute of Health Sciences, Tokyo

The alteration of glycosyltransferase expression and the subsequent changes in oligosaccharide structures are reported in several diseases. The analysis of glycan structural alteration in glycoproteins is becoming increasingly important in the discovery of therapies and diagnostic markers. In this study, we propose a strategy for glycomic/glycoproteomic analysis based on oligosaccharide profiling by LC/MS followed by proteomic approaches, including 2-DE and 2-D lectin blot. As a model of aberrant cells, we used Chinese hamster ovary cells transfected with *N*-acetylglucosaminyltransferase III (GnT-III), which catalyzes the addition of a bisecting *N*-acetylglucosamine (GlcNAc) to β-mannose of the mannosyl core of *N*-linked oligosaccharides. LC/MS equipped with a graphitized carbon column (GCC) enabled us to elucidate the structural alteration induced by the GnT-III expression. Using 2-D lectin blot followed by LC/MS/MS, the protein carrying an extra *N*-acetylhexosamine in cells transfected with GnT-III was successfully identified as integrin α3. Thus, oligosaccharide profiling by GCC-LC/MS followed by proteomic methods can be a powerful tool for glycomic/glycoproteomic analysis.

Received: September 20, 2004
Revised: April 22, 2005
Accepted: April 22, 2005

Keywords:
2DE / LC/MS / Lectin blotting / Oligosaccharides profiling

1 Introduction

It is common knowledge that approximately 50% of proteins in mammalian cells are glycosylated and that glycans play crucial roles in various biological events including cell recognition [1], adhesion [2] and cell-cell interaction [3]. The alteration of glycosyltransferase expression and subsequent changes in oligosaccharide structures are reported in several diseases, including inherited diseases [4], the progression of cancer [5] and autoimmune diseases [6–8]. The analysis of glycan structural alteration in glycoproteins is becoming increasingly important in the discovery of therapies and diagnostic markers.

Comprehensive analysis of proteins in a given cellular sample is the most effective means of elucidating the disease mechanism. Simultaneous separation and characterization of proteins by 2-DE and 2-D LC followed by MS have been utilized as the fundamental approaches to proteomic analysis; however, these approaches alone are ineffectual for the elucidation of the glycan structural alteration in glycoproteins. A strategy based on qualitative and quantitative glycomic analysis is necessary for the study of glycosylation-associated diseases.

LC/MS is widely used for glycosylation analysis in glycoproteins. Previously, we demonstrated that LC/MS equipped with a graphitized carbon column (GCC-LC/MS) is a useful means of oligosaccharide profiling and for the structural analysis of carbohydrates [9–12]. Using this method, oligosaccharides, including high mannose, hybrid and complex

Correspondence: Dr. Nana Kawasaki, 1–18–1, Kamiyoga, Setagaya-ku, Tokyo, 158–8501, Japan
E-mail: nana@nihs.go.jp
Fax: +81-3-3700-9084

Abbreviations: CHO, Chinese hamster ovary; **CHO-III cells**, CHO cells transfected with *N*-acetylglucosaminyltransferase III; **dHex**, deoxyhexose; **GCC**, graphitized carbon column; **GlcNAc**, *N*-acetylglucosamine; **GnT-III**, *N*-acetylglucosaminyltransferase III; **Hex**, hexose; **HexNAc**, *N*-acetylhexosamine; **NeuAc**, *N*-acetylneuraminic acid; **PNGase F**, peptide *N*-glycosidase F

© 2005 WILEY-VCH Verlag GmbH & Co. KGaA, Weinheim

types with or without sialic acids, can be separated, and structural information can be obtained from their mass spectra and chromatographic behavior.

Here we propose a strategy for performing glycomic/glycoproteomic analysis based on a combination of GCC-LC/MS and proteomic approaches.

First, GCC-LC/MS is applied to the analysis of oligosaccharide structural alteration in aberrant cells. Chinese hamster ovary (CHO) cells, used as a model of aberrant cells, were transfected with *N*-acetylglucosaminyltransferase III (GnT-III), which catalyzes the addition of bisecting *N*-acetylglucosamine (GlcNAc) to the trimannosyl core of *N*-linked oligosaccharides [13] and is associated with cell adhesion [14] and the suppression of tumor cell metastasis [15–17]. Then, 2-D lectin blotting followed by LC/MS/MS was used to identify the protein in which glycosylation was altered by the expression of GnT-III.

2 Materials and methods

2.1 Cell lines and culture

The CHO cells were obtained from the Japanese Collection of Research Bioresources (Tokyo, Japan). The human GnT-III cDNA was cloned into the pCI-neo vector. The expression vector was transfected into CHO cells with LipofectAMINE plus reagent, according to the manufacturer's instructions. To screen the transformants, the transfectants were cultured with Ham's F12 medium supplemented with 10% fetal calf serum (FCS) and 1 mg/mL G418. After 2 weeks, the colonies were lifted with a micropipette. A high GnT-III-expressing clone was used in succeeding experiments.

The CHO cells and GnT-III-transfected CHO cells (CHO-III cells) were cultured in Ham's F12 medium supplemented with 10% FCS, 100 U/mL of penicillin and 100 μg/mL of streptomycin under a humidified atmosphere of 95% air and 5% CO_2. After harvesting CHO and CHO-III cells, they were rinsed with PBS containing protease inhibitors and 2 mM EDTA.

2.2 Preparation of insoluble and soluble fractions

The insoluble and soluble fractions were prepared from CHO and CHO-III cells using a Mem-PER Eukaryotic Membrane Protein Extraction Reagent Kit (Pierce Biotechnology, P.O., USA). The detergent in these fractions was removed with Detergent-OUT (Geno Technology, M.O., USA) three times. For desalting and degreasing, seven volumes of acetone were added to the sample solution, and the mixture was stirred and sonicated. The mixture was then incubated at −20°C for 1 h and centrifuged at 4°C for 15 min, 15 000 × g. The supernatants were discarded, and the pellets dried. The protein concentrations were determined using a BCA protein assay kit (Pierce).

2.3 Preparation of *N*-linked oligosaccharide alditols

The protein (500 μg) from each fraction was dissolved in 810 μL of 0.5 M Tris-HCl containing 8 M guanidine-HCl and 5 mM EDTA (pH 8.6), and then 6.0 μL of 2-mercaptoethanol were added in the solution. After incubation at room temperature for 2 h, freshly prepared 0.6 M sodium monoiodoacetamide (135 μL) was added to the solution. After incubation at room temperature for 2 h in the dark, the solution was desalted with PD10 column (Amersham Biosciences, NJ, USA), and the elute was lyophilized. The carboxylmethylated proteins were dissolved in 500 μL of 100 mM PBS (pH 7.2), and 20 U of peptide *N*-glycosidase F (PNGase F) (Roche Diagnostics, Mannheim, Germany) were added to the solution. After incubation at 37°C for 4 days, 1.74 mL of cold ethanol was added to the solution, the mixture was incubated at −20°C for 3 h, and proteins were removed by centrifugation at 4°C for 10 min (15 000 × g). The supernatants containing oligosaccharides were evaporated, and then lyophilized. The oligosaccharides were incubated with 500 μL of 0.5 M $NaBH_4$ at room temperature for 16 h, and then neutralized with 10% (v/v) acetic acid to pH 6.5 and desalted with Envi-Carb (Supelco, Bellefonte, USA).

2.4 GCC-LC/MS

LC was carried out using a MAGIC 2002 system (Michrom BioResources, Auburn, CA, USA). The GCC used was a Hypercarb column (150 × 0.2 mm, ThermoFinnigan, San Jose, CA, USA). The eluents were 5 mM ammonium acetate, pH 8.5, containing 2% ACN (pump A) and 5 mM ammonium acetate, pH 8.5, containing 80% ACN (pump B). The borohydride-reduced oligosaccharides were eluted at a flow rate of 2 μL/min with a gradient of 10–45% of pump B in 90 min. Mass spectra were recorded on a TSQ 7000 triple-stage quadruple mass spectrometer (ThermoFinnigan) equipped with a nanoelectorospray ion source (AMR, Inc., Tokyo, Japan). The mass spectrometer was operated in positive ion mode. Ions in the range of m/z 900–2400 were acquired with a scan duration of 3 s. The ESI voltage was set at 2.0 kV, and the capillary temperature was 175°C. The electron multiplier was set at 1.0 kV. Collisions for MS/MS were carried out with collision energy of 25%, scan duration of 4 s., and mass range of m/z 100–2000.

2.5 1-D SDS-PAGE and lectin blotting

Proteins were separated by 1-D SDS-PAGE (12.5% T, 3% C) as described by Laemmli [18] and stained with SYPRO Orange (Bio-Rad, Richmond, CA, USA) at room temperature for 30 min in transfer buffer (25 mM Tris-HCl, 20 mM glycine and 20% methanol). The gel images were scanned on a Tyhoon 9400 (Amersham Biosciences) at an excitation wavelength of 540/25 nm and an emission wavelength of 590/30 nm. After saving the gel image, the proteins were blotted to a PVDF membrane (Immun-Blot PVDF membrane,

© 2005 WILEY-VCH Verlag GmbH & Co. KGaA, Weinheim

0.2 μm, Bio-Rad) at 3.0 mA/cm^2, 20 V for 30 min in transfer buffer containing 0.1% SDS using a semi-dry blotter (Trans-blot SD sel, Bio-Rad). The efficiency and position of the transfer were confirmed using SYPRO Orange transferred together with proteins. Nonspecific sites on the membrane were blocked at 4°C for 16 h in 0.5% casein-PBS. After the membranes were washed with 0.05% Tween-PBS (T-PBS) three times, they were treated with 0.1 U/mL of sialidase (Nacalai Tesque, Kyoto, Japan) at 37°C for 16 h in 0.5 M acetate buffer (pH 5.0). The membranes were then re-blocked with 0.5% casein-PBS at 37°C for 15 min, washed with T-PBS three times, and incubated with biotinylated phytohemagglutinin-E4 (PHA-E4, 2 μg/mL) at 4°C for 2 h in PBS (pH 7.4). The membranes were then washed with T-PBS and incubated with 1:1000 diluted avidin-alkaline phosphatase (AP) complex solution at 4°C for 1 h in PBS.

2.6 Concentration of target proteins in the gel

The band detected by lectin blotting on 1-D gel was excised and then mashed in 20 mM Tris-HCl (pH 8.0) containing 2% SDS. The proteins in the gel particles were extracted by intermittent sonication at 4°C for 30 min, followed by shaking at room temperature for 16 h. After extraction, the gel particles were removed by centrifugation (15 000 × g). The proteins in the supernatant were precipitated with sevenfold acetone at −20°C for 3 h, and then the precipitates were washed with acetone three times to remove salts and detergent.

2.7 2-DE

For first dimension IEF of the sample, Immobiline DryStrip gel (13 cm, pH4–7 NL, Amersham Biosciences) was used. The samples were dissolved in IEF solution containing 7 M urea, 2 M thiourea, 18 mM DTT, 0.5% IPG buffer, 2% CHAPS, and bromophenol blue. Dried IPG strips were rehydrated overnight in the sample solution. IEF was then performed using the following steps: 500 V for 1 h, 100 V for 1 h, and 8000 V for 2 h, *i.e.* a total of 17.5 kVh.

IPG strips were treated with 10 mL of 50 mM Tris-HCl (pH 8.8) containing 2% SDS, 6 M urea, 30% glycerol and 65 mM DTT for 15 min, and then treated with 10 mL of 50 mM Tris-Cl (pH 8.8) containing 2% SDS, 6 M urea, 30% glycerol and 135 mM iodoacetamide for 15 min in order to reduce the disulfide bonds of cysteinyl residues. SDS-polyacrylamide gels (7.5%T, 3%C, size 140 × 140 × 1 mm) and running buffer containing 25 mM Tris-HCl, 192 mM glycine and 0.1% SDS were used for the 2-DE. The gels were run at 25 mA/gel after setting the IPG strip on the gel. Fluorescent staining and scanning of gel, followed by lectin blotting, were performed as mentioned above. In 2-D lectin blotting, the proteins were blotted to a PVDF membrane at 3.0 mA/cm^2, 20 V for 90 min.

2.8 In-gel digestion and protein identification by LC/MS/MS

Interesting spots were excised from the 2-DE gel for in-gel trypsin digestion. The gel particles were destained with 20 mM ammonium bicarbonate containing 50% methanol in microcentrifuge tubes, and dehydrated in 100% ACN. Enzymatic digestion was performed overnight at 37°C with 5 μL of 20 μg/mL trypsin (Promega, Madison, WI, USA) in 20 mM ammonium bicarbonate (pH 8.5). Digested peptides were extracted with 1% TFA in 50% ACN, and samples were dried with a Speed-Vac and redissolved in 0.1% TFA for LC/MS.

LC was carried out using a Paradigm MS4 (Michrom BioResources) equipped with Magic C18 column (50 × 0.2 mm, Michrom BioResources). The eluents were 0.1% formic acid containing 2% ACN (pump A), and 0.1% formic acid containing 90% ACN (pump B). The peptides were eluted at a flow rate of 2 μL/min with a gradient of 5–70% of pump B in 30 min. Mass spectra were recorded on an API QSTAR Pulsar i (Applied Biosystems, Foster City, CA, USA) in the positive ion mode. The proteins were identified by searching the Swiss-Prot database using MASCOT (Matrix Science, UK). The mass range and MS/MS range were *m/z* 400–2000 and *m/z* 100–2000, respectively, and the ESI voltage was set at 2.5 kV.

3 Results

3.1 Analysis of glycans in the insoluble fractions

N-linked oligosaccharides were released from soluble and insoluble fractions by PNGase F and reduced with $NaBH_4$ to prevent the separation of anomers by GCC. Figure 1A shows the *N*-linked oligosaccharide profile of the insoluble fraction from CHO cells (5 × 10^7). Diverse oligosaccharide ions were detected by full scan in the positive ion mode of MS. Oligosaccharides were numbered with the labels on peaks where they were detected, and the multiple oligosaccharides in single peak were classified by the digits behind alphabets, such as peaks A1 and A2. Their monosaccharide compositions were deduced from the *m/z* values as shown in Table 1. *N*-linked oligosaccharides from CHO cells have a high proportion of high mannose-type and bi-, tri- and tetra-antennary complex type oligosaccharides [19, 20]. High mannose-type oligosaccharides, $[Man]_{5-9}[GlcNAc]_2$ were detected at 9–23 min (peaks A–E and K). Major components (peaks N2, Q2, R1, S1, T1, U1 and V2) were deduced as fucosylated and non-fucosylated biantennary forms with mono- and di-sialic acids from previous articles and their monosaccharide compositions. Various oligosaccharides, including mono- (peak N1 and Q1), tri- (peak P1, U2, V1), tetra-antennary (peak V3), and hybrid-type (peak F1 and I1) oligosaccharides were detected as minor components together with low molecular weight oligosaccharides such as the trimannosyl core (peaks G1 and O1).

© 2005 WILEY-VCH Verlag GmbH & Co. KGaA, Weinheim

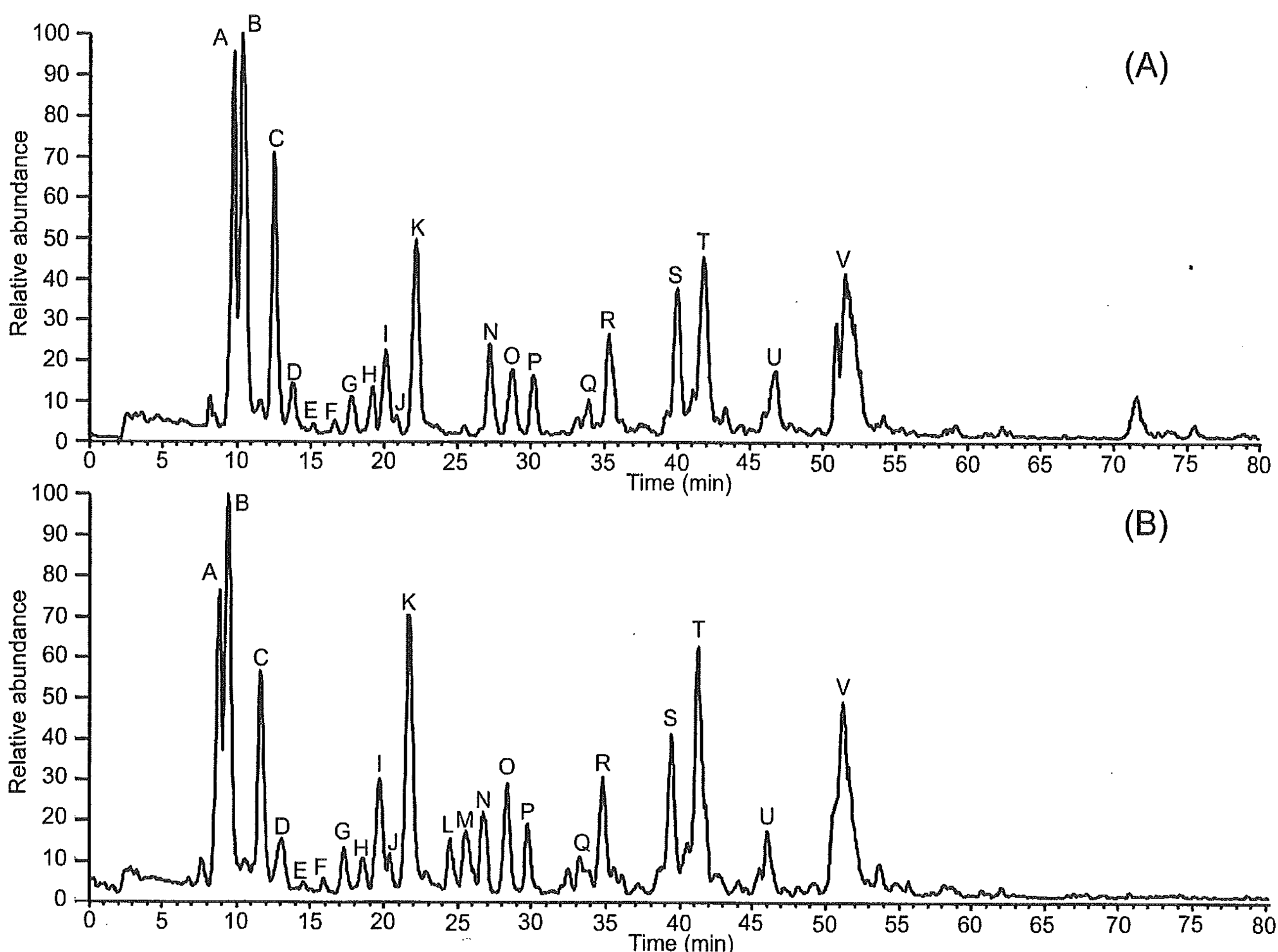

Figure 1. Total ion chromatograms of GCC-LC/MS of borohydride-reduced *N*-linked oligosaccharides released from insoluble fraction of CHO (A) and CHO-III (B) in positive ion mode. Pump A: 5 mM ammonium acetate, pH 8.5, containing 2% ACN. Pump B: 5 mM ammonium acetate, pH 8.5, containing 80% ACN. The borohydride-reduced oligosaccharides were eluted at a flow rate of 2 μL/min with a gradient of 10–45% of pump B in 90 min.

Figure 1B shows the oligosaccharide profile of the CHO-III-insoluble fraction. The distribution of oligosaccharides in CHO-III was different from that in the CHO cell insoluble fraction. Some additional peaks (peaks L1 and M1) were detected in the CHO-III-insoluble fraction, and their doubly charged ions at *m/z* 1143.2 and 1143.0 were consistent with the theoretical *m/z* values of fucosylated biantennary-bearing NeuAc with one additional HexNAc. Figure 2 shows the MS/MS spectrum of peak M1. Detection of $B_{1\gamma}/Y_6^{2+}$ at *m/z* 894.1 and an intense ion of $[HexNAc]^+$, at *m/z* 204 suggest that the oligosaccharide (peak M1) carries one GlcNAc at either of the non-reducing ends. Peak M1 is possibly assigned to bisected biantennary form. In addition, peaks D1, I2 and S2, which were not found in the profile of CHO, were detected in that of CHO-III (Fig. 1B). They can also be deduced as bisected biantennary forms from their MS/MS spectra. Other than these oligosaccharides bearing GlcNAc at either of the non-reducing ends in CHO-III cells, there was no significant difference in glycosylation between CHO and CHO-III cells. These results suggest that only limited oligosaccharides are altered by the expression of GnT-III.

3.2 Analysis of glycans in the soluble fractions

Figure 3A and B shows the *N*-linked oligosaccharide profiles of the soluble fractions of CHO and CHO-III, respectively. The oligosaccharide components of soluble fractions are very different from those of insoluble fractions (Table 1). High mannose-type oligosaccharides, $[Man]_{5-9}[GlcNAc]_2$, were detected as major components (peaks A–C and K), and complex-type and hybrid-type oligosaccharides were detected as minor oligosaccharides in the soluble fraction. Oligosaccharides bearing extra GlcNAc (D1, L1 and M1) were also detected in the soluble fraction of CHO-III.

© 2005 WILEY-VCH Verlag GmbH & Co. KGaA, Weinheim

Table 1. Observed *m/z* values and carbohydrate compositions of peaks A-V in total ion chromatogram 3 of CHO-insoluble (Fig. 1A), CHO-III-insoluble (Fig. 1B), CHO-soluble (Fig. 3A) and CHOIII-soluble (Fig. 3B) fractions

Carbohydrate composition[a)]	Theoretical mass[b)]	Peak No.		Insoluble fraction				Soluble fraction			
				CHO		CHO-III		CHO		CHO-III	
				Charge state	Observed *m/z*	Charge state	Observed *m/z*	Charge state	Observed *m/z*	Charge state	Observed *m/z*
[Hex]$_7$[HexNAc]$_2$	1561.4	A	A1	H^+	1562.2	H^+	1562.0	Na^+	1584.4	Na^+	1584.2
[Hex]$_8$[HexNAc]$_2$	1723.5		A2	Na^+	1746.3	Na^+	1746.3	Na^+	1746.5	Na^+	1746.1
[Hex]$_9$[HexNAc]$_2$	1885.7	B	B1	Na^+	1908.4	Na^+	1908.5	Na^+	1908.4	Na^+	1908.9
[Hex]$_6$[HexNAc]$_2$	1399.3	C	C1	H^+	1400.1	H^+	1400.0	H^+	1399.7	H^+	1399.9
[Hex]$_7$[HexNAc]$_2$	1561.4		C2	Na^+	1584.2	Na^+	1584.0	Na^+	1584.8	Na^+	1584.0
[dHex]$_1$[Hex]$_5$[HexNAc]$_5$	1992.9	D	D1		N.D.[c)]	$2H^+$	**997.4**		N.D.	$2H^+$	**997.5**
[Hex]$_6$[HexNAc]$_2$	1399.3		D2	Na^+	1422.0	Na^+	1421.9		N.D.		N.D.
[Hex]$_7$[HexNAc]$_2$	1561.4		D3	Na^+	1584.2	Na^+	1584.1		N.D.		N.D.
[Hex]$_8$[HexNAc]$_2$	1723.5		D4	Na^+	1746.2	Na^+	1746.4		N.D.		N.D.
[Hex]$_4$[HexNAc]$_2$	1075.0	E	E1	Na^+	1097.9	Na^+	1097.6		N.D.		N.D.
[Hex]$_6$[HexNAc]$_2$	1399.3		E2	H^+	1400.1	H^+	1400.0		N.D.		N.D.
[Hex]$_6$[HexNAc]$_3$	1602.5	F	F1	H^+	1604.0	H^+	1603.1		N.D.		N.D.
[Hex]$_3$[HexNAc]$_2$	912.8	G	G1	H^+	913.7	H^+	913.7	Na^+	935.7	Na^+	935.6
[Hex]$_5$[HexNAc]$_4$	1643.5	H	H1	H^+	1644.5	H^+	1644.2	Na^+	1666.3	Na^+	1666.4
[Hex]$_6$[HexNAc]$_4$	1827.6	I	I1	$2Na^+$	914.7	$2Na^+$	914.7		N.D.		N.D.
[Hex]$_5$[HexNAc]$_5$[NeuAc]$_1$	2137.9		I2		N.D.	$2H^+$	**1069.8**		N.D.		N.D.
[dHex]$_1$[Hex]$_3$[HexNAc]$_4$	1465.4	J	J1	H^+	1466.1	H^+	1466.1	Na^+	1488.2	Na^+	1487.9
[Hex]$_5$[HexNAc]$_2$	1237.1	K	K1	H^+	1238.0	H^+	1238.0	H^+	1237.9	H^+	1237.9
[dHex]$_1$[Hex]$_5$[HexNAc]$_5$[NeuAc]$_1$	2284.1	L	L1		N.D.	$2H^+$	**1143.2**		N.D.	$2H^+$	**1142.9**
[dHex]$_1$[Hex]$_5$[HexNAc]$_5$[NeuAc]$_1$	2284.1	M	M1		N.D.	$2H^+$	**1143.0**		N.D.	$2H^+$	**1143.3**
[dHex]$_1$[Hex]$_4$[HexNAc]$_3$	1424.3	N	N1	H^+	1425.4	H^+	1425.3	Na^+	1447.1	Na^+	1447.1
[dHex]$_1$[Hex]$_5$[HexNAc]$_4$	1789.7		N2	H^+	1790.1	H^+	1790.3	Na^+	1812.3	Na^+	1812.1
[dHex]$_1$[Hex]$_3$[HexNAc]$_2$	1059.0	O	O1	H^+	1059.7	H^+	1059.7	H^+	1059.8	H^+	1059.7
[dHex]$_1$[Hex]$_6$[HexNAc]$_5$	2155.0	P	P1	$2H^+$	1078.5	$2H^+$	1078.5		N.D.		N.D.
[dHex]$_1$[Hex]$_3$[HexNAc]$_3$	1262.2	Q	Q1	H^+	1263.0	H^+	1263.0		N.D.		N.D.
[Hex]$_5$[HexNAc]$_4$[NeuAc]$_1$	1934.7		Q2	$2H^+$	968.4	$2H^+$	968.4		N.D.		N.D.
[Hex]$_5$[HexNAc]$_4$[NeuAc]$_1$	1934.7	R	R1	$2H^+$	968.4	$2H^+$	968.4	$2H^+$	968.7	$2H^+$	968.2
[dHex]$_1$[Hex]$_5$[HexNAc]$_4$[NeuAc]$_1$	2080.9	S	S1	$2H^+$	1041.4	$2H^+$	1041.4	$2H^+$	1041.4	$2H^+$	1041.3
[dHex]$_1$[Hex]$_5$[HexNAc]$_5$[NeuAc]$_2$	2574.0		S2		N.D.	$2H^+$	**1288.5**		N.D.		N.D.
[dHex]$_1$[Hex]$_5$[HexNAc]$_4$[NeuAc]$_1$	2080.9	T	T1	$2H^+$	1041.4	$2H^+$	1041.5	$2H^+$	1041.4	$2H^+$	1041.3
[Hex]$_5$[HexNAc]$_4$[NeuAc]$_2$	2226.0	U	U1	$2H^+$	1114.0	$2H^+$	1113.9	$2H^+$	1113.9	$2H^+$	1113.9
[dHex]$_1$[Hex]$_6$[HexNAc]$_5$[NeuAc]$_1$	2446.2		U2	$2H^+$	1224.2	$2H^+$	1224.3	$2Na^+$	1124.9		N.D.
[dHex]$_1$[Hex]$_6$[HexNAc]$_5$[NeuAc]$_2$	2737.5	V	V1	$2H^+$	1370.0	$2H^+$	1370.0		N.D.		N.D.
[dHex]$_1$[Hex]$_5$[HexNAc]$_4$[NeuAc]$_2$	2372.1		V2	$2H^+$	1187.1	$2H^+$	1187.1	$2H^+$	1187.2	$2H^+$	1187.2
[dHex]$_1$[Hex]$_7$[HexNAc]$_6$[NeuAc]$_1$	2811.6		V3	$2H^+$	1406.8	$2H^+$	1406.6		N.D.		N.D.

The characteristic *m/z* values observed in total ion chromatograms of CHO-III are depicted in bold type.

a) [dHex], deoxyhexose; [Hex], hexose; [HexNAc], *N*-acetylhexosamine; [NeuAc], *N*-acetylneuraminic acid.

b) Monoisotopic mass values.

c) Not detected.

© 2005 WILEY-VCH Verlag GmbH & Co. KGaA, Weinheim

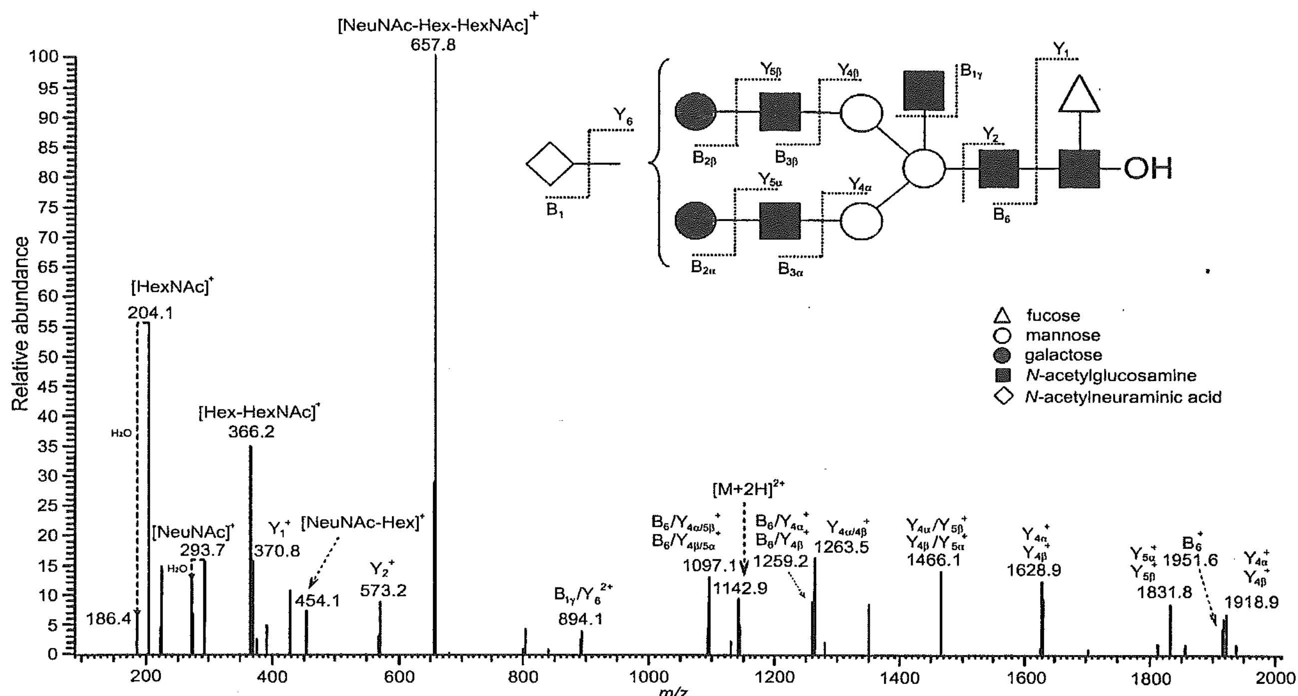

Figure 2. MS/MS spectrum of fucosylated biantennary *N*-linked oligosaccharide (peak M1) detected in the insoluble fraction from CHO-III.

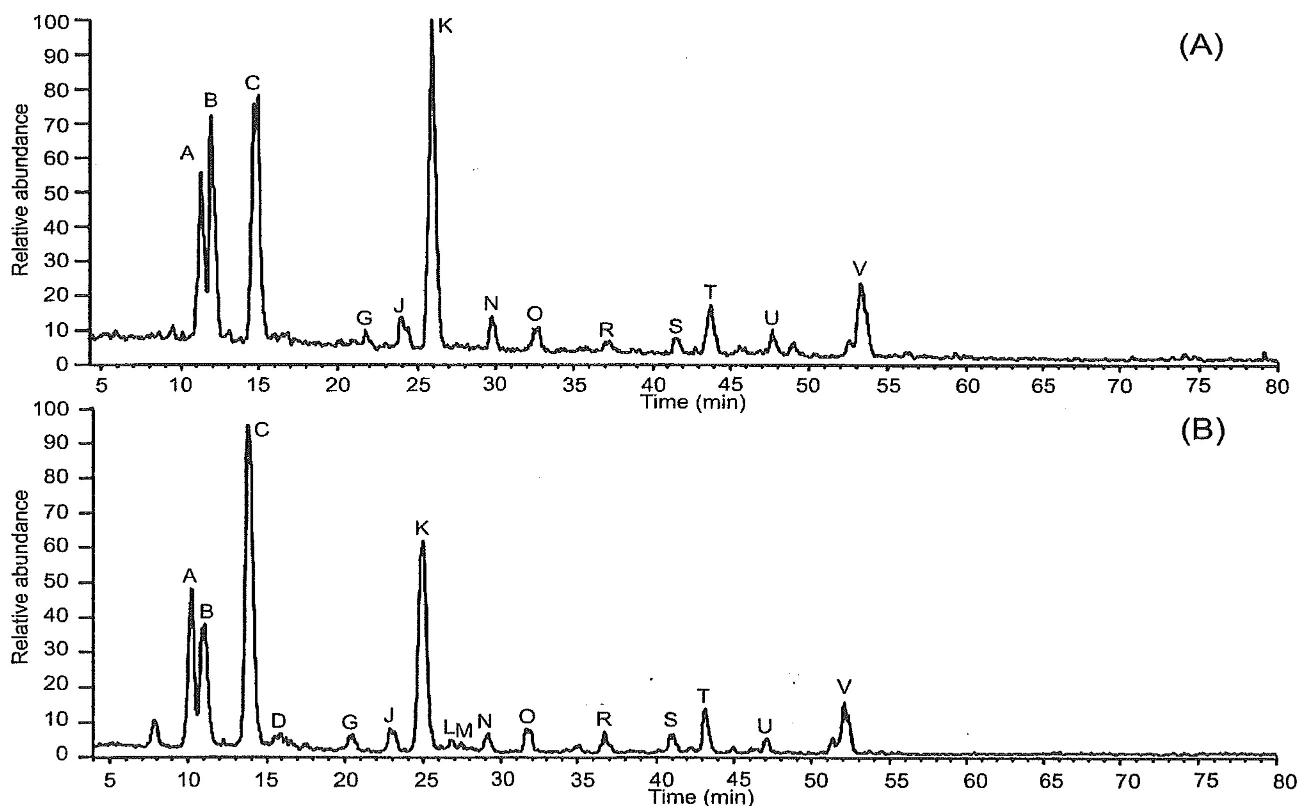

Figure 3. Total ion chromatograms of GCC-LC/MS of borohydride-reduced *N*-linked oligosaccharides released from the soluble fractions of CHO (A) and CHO-III (B) in positive ion mode. Pump A: 5 mM ammonium acetate, pH 8.5, containing 2% ACN. Pump B: 5 mM ammonium acetate, pH 8.5, containing 80% ACN. The borohydride-reduced oligosaccharides were eluted at a flow rate of 2 μL/min with a gradient of 10–45% of pump B in 90 min.

© 2005 WILEY-VCH Verlag GmbH & Co. KGaA, Weinheim

3.3 Identification of protein bearing bisected oligosaccharides

To identify proteins with altered glycans by the expression of GnT-III, we performed 2-DE followed by lectin blotting using PHA-E4 lectin, which recognizes bisecting GlcNAc in complex-type oligosaccharides. Although some bisected glycoproteins (70–120 kDa) could be visualized by 2-D lectin blotting, their expressions were too low to be detected on 2-DE gel. Lectin affinity chromatography, which is generally used for the concentration of glycoproteins, cannot be used for the insoluble fraction due to the presence of detergent in the solvent medium. Therefore, we first performed 1-D SDS-PAGE followed by lectin blotting, and then proteins in the range of 70–120 kDa were extracted from the gel (Fig. 4). 2-DE followed by lectin blotting was then performed, and interesting spots were successfully detected on 2-DE gel. Figure 5A and B shows the 2-DE gel images and the 2-D lectin blot of extracted proteins, respectively. The remarkable train spots (120 Da) of glycoprotein were picked up and in-gel digested with trypsin. The digest was subjected to LC/MS/MS, and the integrin α3 precursor was identified as the GnT-III target protein.

4 Discussion

The development of a simple and rapid method to explore glycan structural alteration in a complex mixture is required to elucidate the mechanisms of diseases involving glycan alteration. In this study, we demonstrated that GCC-LC/MS, which is used for glycosylation analysis in glycoproteins, is

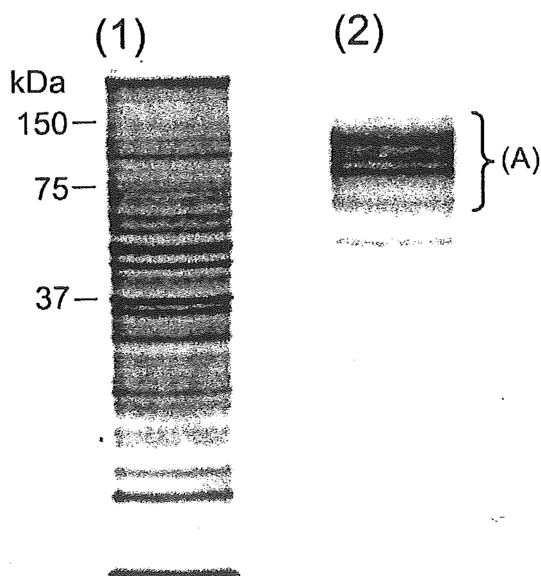

Figure 4. (1) 1-D SDS-PAGE and (2) lectin blot images of the CHO-III insoluble fraction. Proteins were separated on a 12.5% SDS-PAGE gel and stained with SYPRO Orange.

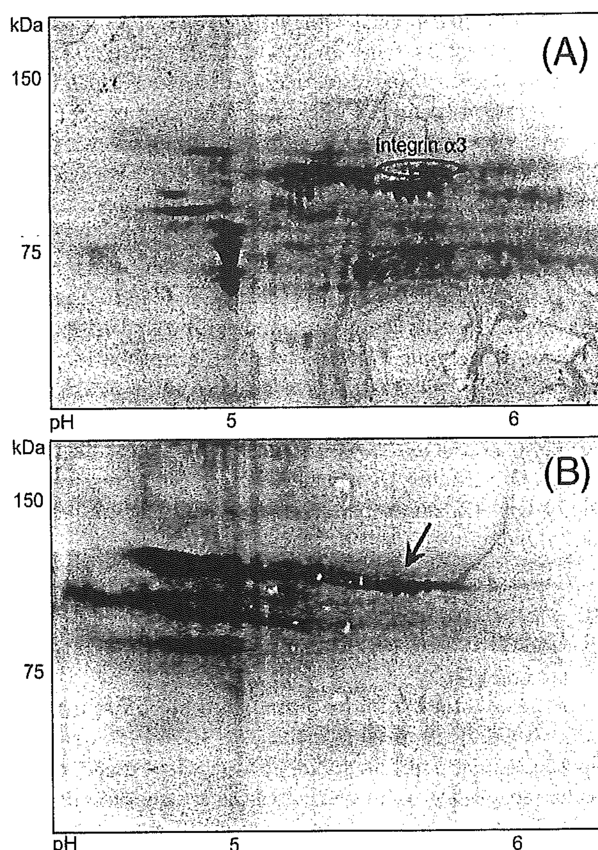

Figure 5. Enlarged partial (A) 2-DE and (B) lectin blot images from band A in Fig. 4.

applicable for the exploration of changes in glycosylation between samples. Using GCC-LC/MS, high mannose, hybrid, and complex types as well as neutral and acidic oligosaccharides could be separated and characterized by a single analysis. GCC-LC/MS clearly shows differences in glycosylation between soluble and insoluble fractions. High mannose-type oligosaccharides were detected as major components in the soluble fraction. The soluble fraction contains endoplasmic reticulum and Golgi apparatus, where *N*-linked oligosaccharides are constructed. The predominance of high-mannose-type oligosaccharides in the soluble fraction may be the cause of immature oligosaccharides in the process of biosynthesis. In contrast, complex and hybrid types with or without sialic acids were detected in the insoluble fraction, suggesting that membrane proteins carry mature oligosaccharides.

In addition, GCC-LC/MS revealed differences in glycosylation between control cells and aberrant model cells. Biantennary forms bearing extra GlcNAc were obviously increased in cells transfected with the GnT-III gene, indicating that our methodology allows us to explore changes in the glycosyltransferase expression followed by glycan alteration. Although MS is frequently used for the analysis of glycosylation, identification of oligosaccharide isomers by MS alone

© 2005 WILEY-VCH Verlag GmbH & Co. KGaA, Weinheim

still remains challenges. Positional isomers could be differentiated by multiple-stage tandem mass spectrometry (MS^n); however, MS^n itself failed to identify oligosaccharides if the sample contained positional isomers. The use of GCC-LC/MS enables us to differentiate the structural isomers and perform differential analysis in glycosylation between normal and aberrant cells.

GnT-III is reported to involve the suppression of tumor cell metastasis and is assumed to be a marker of cancerous alteration in hepatic carcinoma [21, 22]. To identify the protein in which glycosylation was modified by GnT-III expression, we carried out 2-DE followed by lectin blotting, and Integrin α3 was identified as a target protein of GnT-III. Integrin α3, a type I membrane protein, is known to be a receptor of adhesion molecules, such as laminin 5 and 10/11 [23–25]. Our finding, in which integrin α3 is a target molecule of GnT-III, might be a clue to clarify the suppression mechanism of metastasis by GnT-III.

5 Concluding remarks

We propose a strategy for glycomic/glycoproteomic analysis using GCC-LC/MS in Fig. 6. First, GCC-LC/MS is used for oligosaccharide profiling to identify disease-related oligosaccharides. Based on the carbohydrate structure, appropriate lectins or antibodies could be selected for western blotting. Proteins carrying disease-related oligosaccharides could then be identified by 2-D lectin blotting followed by MS/MS analysis. Using several groups, 2-D lectin blotting has been proposed for the characterization of glycoproteins on gel [26, 27]. The use of mass spectrometric oligosaccharide profiling, which can directly characterize glycan structures, is worthwhile to obtain structural information about disease-related carbohydrate and is helpful in the subsequent choice of appropriate lectins and antibodies. Our method is expected to be a powerful tool for glycomic/glycoproteomic analysis.

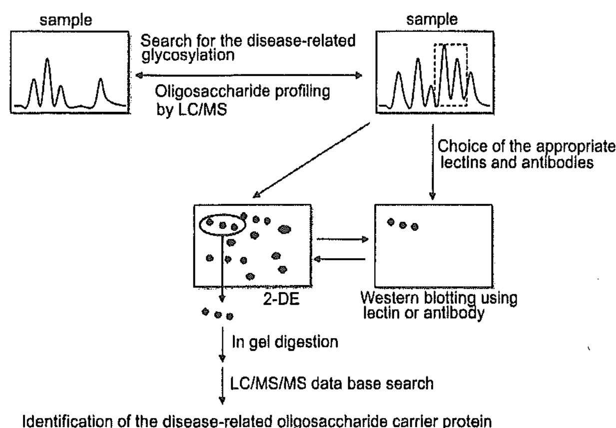

Figure 6. Strategy for glycomics/glycoproteomics using GCC-LC/MS, 2-DE and 2-D Western blotting using lectin or antibody.

6 References

[1] Varki, A., *Glycobiology* 1993, *3*, 97–130.

[2] Isaji, T., Gu, J., Nishiuchi, R., Zhao, Y. *et al.*, *J. Biol. Chem.* 2004, *279*, 19747–19754.

[3] Stanley, P., *Biochim. Biophys. Acta* 2002, *1573*, 363–368.

[4] Schachter, H., *Cell Mol. Life Sci.* 2001, *58*, 1085–1104.

[5] Dennis, J. W., Granovsky, M., Warren, C.E., *Biochim. Biophys. Acta* 1999, *1473*, 21–34.

[6] Delves, P. J., *Autoimmunity* 1998, *27*, 239–253.

[7] Gleeson, P. A., *Biochim. Biophys. Acta* 1994, *1197*, 237–255.

[8] Chui, D., Sellakumar, G., Green, R., Sutton-Smith, M. *et al.*, *Proc. Natl. Acad. Sci. USA* 2001, *98*, 1142–1147.

[9] Itoh, S., Kawasaki, N., Ohta, M., Hyuga, M. *et al.*, *J. Chromatogr. A* 2002, *968*, 89–100.

[10] Kawasaki, N., Haishima, Y., Ohta, M., Itoh, S. *et al.*, *Glycobiology* 2001, *11*, 1043–1049.

[11] Kawasaki, N., Ohta, M., Itoh, S., Hyuga, M. *et al.*, *Biologicals* 2002, *30*, 113–123.

[12] Davies, M., Smith, K. D., Harbin, A. M., Hounsell, E. F., *J. Chromatogr.* 1992, *609*, 125–131.

[13] Narasimhan, S., *J. Biol. Chem.* 1982, *257*, 10235–10242.

[14] Yoshimura, M., Ihara, Y., Matsuzawa, Y., Taniguchi, N., *J. Biol. Chem.* 1996, *271*, 13811–13815.

[15] Taniguchi, N., Miyoshi, E., Ko, J. H., Ikeda, Y., Ihara, Y., *Biochim. Biophys. Acta* 1999, *1455*, 287–300.

[16] Yoshimura, M., Nishikawa, A., Ihara, Y., Taniguchi, S., Taniguchi, N., *Proc. Natl. Acad. Sci. USA.*1995, *92*, 8754–8758.

[17] Bhaumik, M., Harris, T., Sundaram, S., Johnson, L. *et al.*, *Cancer Res.* 1998, *58*, 2881–2887.

[18] Laemmli, U. K., *Nature* 1970, *227*, 680–685.

[19] Stanley, S., Sundaram, S., Tang, J., Shi, S., *Glycobiology* 2005, *15*, 43–53.

[20] Lee, J., Sundaram, S., Shaper, N. L., Raju, S., Stanley, P., *J. Biol .Chem.* 2001, *276*, 13924–13934.

[21] Yamashita, K., Koide, N., Endo, T., Iwaki, Y., Kobata, A., *J. Biol. Chem.* 1989, *264*, 2415–2423.

[22] Yamashita, K., Hitoi, A., Taniguchi, N., Yokosawa, N. *et al.*, *Cancer Res.* 1983, *43*, 5059–5063.

[23] Carter, W. G., Ryan, M. C., Gahr, P. J., *Cell* 1991, *65*, 599–610.

[24] Kikkawa, Y., Umeda, M., Miyazaki, K., *J. Biochem (Tokyo)* 1994, *116*, 862–869.

[25] Kikkawa, Y., Sanzen, N., Sekiguchi, K., *J. Biol. Chem.* 1998, *273*, 15854–15859.

[26] Kim, Y. S., Hwang, S. Y., Oh, S., Shon, H. *et al.*, *Proteomics* 2004, *4*, 3353–3358.

[27] Rahman, M. A., Karsani, S. A., Othman, I., Rahman, P. S. A., Hashim, O. H., *Biochem. Biophys. Res. Commun.* 2002, *295*, 1007–1013.

© 2005 WILEY-VCH Verlag GmbH & Co. KGaA, Weinheim

ELSEVIER

Available online at www.sciencedirect.com
SCIENCE DIRECT®

Journal of Chromatography A, 1094 (2005) 105–117

JOURNAL OF
CHROMATOGRAPHY A

www.elsevier.com/locate/chroma

Characterization of a gel-separated unknown glycoprotein by liquid chromatography/multistage tandem mass spectrometry Analysis of rat brain Thy-1 separated by sodium dodecyl sulfate-polyacrylamide gel electrophoresis

Satsuki Itoh [a], Nana Kawasaki [a,b,*], Akira Harazono [a], Noritaka Hashii [a], Yukari Matsuishi [b], Toru Kawanishi [a], Takao Hayakawa [a]

[a] *Division of Biological Chemistry and Biologicals, National Institute of Health Science, 1-18-1, Kamiyoga, Setagaya-ku, Tokyo 158-8501, Japan*
[b] *CREST, Japan Science and Technology Agency (JST), Japan*

Received 17 May 2005; received in revised form 17 July 2005; accepted 25 July 2005
Available online 5 October 2005

Abstract

We developed an efficient and convenient strategy for protein identification and glycosylation analysis of a small amount of unknown glycoprotein in a biological sample. The procedure involves isolation of proteins by electrophoresis and mass spectrometric peptide/glycopeptide mapping by LC/ion trap mass spectrometer. For the complete glycosylation analysis, proteins were extracted in intact form from the gel, and proteinase-digested glycoproteins were then subjected to LC/multistage tandem MS (MS^n) incorporating a full mass scan, in-source collision-induced dissociation (CID), and data-dependent MS^n. The glycopeptides were localized in the peptide/glycopeptide map by using oxonium ions such as $HexNAc^+$ and $NeuAc^+$, generated by in-source CID, and neutral loss by CID-MS/MS. We conducted the search analysis for the glycopeptide identification using search parameters containing a possible glycosylation at the Asn residue with *N*-acetylglucosamine (203 Da). We were able to identify the glycopeptides resulting from predictable digestion with proteinase. The glycopeptides caused by irregular cleavages were not identified by the database search analysis, but their elution positions were localized using oxonium ions produced by in-source CID, and neutral loss by the data-dependent MS^n. Then, all glycopeptides could be identified based on the product ion spectra which were sorted from data-dependent CID-MS^n spectra acquired around localized positions. Using this strategy, we successfully elucidated site-specific glycosylation of Thy-1, glycosylphosphatidylinositol (GPI)-anchored proteins glycosylated at Asn23, 74, and 98, and at Cys111. High-mannose-type, complex-type, and hybrid-type oligosaccharides were all found to be attached to Asn23, 74 and 98, and four GPI structures could be characterized. Our method is simple, rapid and useful for the characterization of unknown glycoproteins in a complex mixture of proteins.
© 2005 Elsevier B.V. All rights reserved.

Keywords: Glycoprotein; LC/MS; Ion trap mass spectrometer; In-source CID; Thy-1

1. Introduction

Glycosylation is one of the most abundant post-translational modifications of proteins [1]. Most glycoproteins exist in heterogeneous forms due to their carbohydrate heterogeneity at multiple glycosylation sites. Because heterogeneity at each glycosylation site can be associated with many biological functions [2,3], it is necessary to analyze the oligosaccharide structures at each glycosylation site.

Mass spectrometric peptide/glycopeptide mapping by liquid chromatography coupled with electrospray ionaization tandem mass spectrometry (LC/ESI-MS/MS) is now used for characterization of glycoproteins [4,5]. Site-specific glycosylation of some gel-separated glycoproteins can be analyzed by in-gel proteinase digestion followed by MS; this method, however, gives unsatisfactory results due to a lower recovery of some glycopeptides from the gel [6–8]. For

* Corresponding author. Tel.: +81 3 3700 1141; fax: +81 3 3707 6950.
E-mail address: nana@nihs.go.jp (N. Kawasaki).

0021-9673/$ – see front matter © 2005 Elsevier B.V. All rights reserved.
doi:10.1016/j.chroma.2005.07.100

complete site-specific glycosylation analysis, all glycopeptide fragments should be recovered from the gel. Hence, the extraction of a whole glycoprotein from the gel before proteinase digestion would be more reasonable than in-gel digestion. Additionally, the poor ionization efficiency of glycopeptides makes it difficult to analyze the glycosylation of glycopeptides in a complex mixture of peptides [6,9]. The glycopeptide-specific method is required for mass spectrometric peptide/glycopeptide mapping.

A precursor ion scan using triple quadrupole-type mass spectrometer is favorably used for analysis of glycopeptides [10–13]. However, this method requires repetitive analysis for the protein identification and glycosylation analysis, as it monitors carbohydrate marker ions such as $HexNAc^+$ and $Hex\text{-}HexNAc^+$ fragmented from glycopeptides by collision-induced dissociation (CID)-MS/MS, and does not provide product ion spectra of non-glycosylated peptides. As such, additional analysis would not be possible for small quantities of proteins, including gel-separated glycoproteins. As an alternative method, we have previously demonstrated peptide/glycopeptide mapping using quadrupole time-of-flight mass spectrometer, by which product ions arise from both peptides and carbohydrates [14]. Using oxonium ions as marker ions, we can sort out product ion spectra of glycopeptides from a number of product ion spectra of peptides, and can determine the amino acid sequences of glycopeptides, glycosylation sites, and monosaccharide composition in a single analysis. Recently, ion trap mass spectrometry (ITMS), which is capable of data-dependent multistage tandem MS (MS^n), has been found to be preferable for use in glycosylation analysis of glycopeptides [15,16]. Glycopeptide-specific detection by precursor ion scan and data-dependent scan cannot be used for glycosylation analysis by ITMS due to the low mass cut-off system. Instead, oxonium ions fragmented by in-source CID are used for the localization of glycopeptides in the peptide/glycopeptide map [3,17]. It has recently been reported that peptide + GlcNAc ions originating from *N*-glycosylated peptides by MS^2 yield peptide b and y ions by further MS^n, and that the peptide sequence and *N*-glycosylation sites can be identified based on the peptide fragment ions [15,16,18]. In addition, another group has reported that glycopeptides can be identified in peptide/glycopeptide map by a search analysis using a database to which all possible cleavage products of the glycopeptides have been added in advance [19]. A combination of peptide/glycopeptide mapping with in-source CID, data-dependent CID-MS^n, and the database search analysis would enable protein identification, glycopeptide selection, and glycosylation analysis of a small amount of glycoprotein.

In the present study, we developed a strategy for the characterization of a small amount of unknown glycoprotein in a biological sample. An unknown glycoprotein was isolated by electrophoresis and extracted from the gel in an intact form. We used sodium dodecyl sulfate (SDS), which is effective for extracting proteins from the gel, and could be easily removed by adding cold acetone. The proteinase-digested glycoprotein was subjected to peptide/glycopeptide mapping, with the sequential scan consisting of a full mass scan, in-source CID, and data-dependent CID-MS^n. Using this method, we carried out site-specific glycosylation analysis of glycosylphosphatidylinositol (GPI)-anchored proteins in rat brain. A computer database search was used for the identification of a GPI-anchored protein and its *N*-glycosylation sites. In-source CID and data-dependent CID-MS/MS were also used for localization of peptides with *N*-glycan and GPI in the peptide/glycopeptide map. On the basis of their product ion spectra, we elucidated *N*-glycosylation at each glycosylation site and the structure of GPIs.

2. Experimental

2.1. Materials

Rat brains were purchased from Nippon SLC (Hamamatsu, Japan). Trypsin-Gold and endoproteinase Asp-N were purchased from Promega (Madison, WI, USA) and Wako Pure Chemical (Osaka, Japan), respectively. Phosphatidylinositol-specific phospholipase C (PIPLC) from *Bacillus cereus* were purchased from Molecular Probes (Eugene, OR, USA). All other chemicals used were of the highest purity available.

2.2. Sodium dodecyl sulfate-polyacrylamide gel electrophoresis (SDS-PAGE) of PIPLC-treated GPI-anchored proteins

PIPLC-treated GPI-anchored proteins were prepared from rat brain utilizing Triton X-114 phase partition and PIPLC digestion [20,21]. Two whole rat brains (2.8 g, Wistar, male, 3 weeks) were homogenized in cold acetone and centrifuged for 10 min at 4 °C. The precipitate was then homogenized in $CHCl_3$: methanol (2:1, v/v) and centrifuged for 10 min at 4 °C. After being washed with methanol, the pellet was homogenized in 50 mM Tris–HCl (pH 7.4) containing 150 mM NaCl, 1 mM ethylenediaminetetraacetic acid (EDTA), and 1 mM phenylmethylsulfonyl fluoride (PMSF), and centrifuged at 10,000 × *g* at 4 °C for 20 min. The pellet was resuspended in the same buffer with an additional 2% Triton X-114 (v/v), and stirred at 4 °C for 16 h. After centrifugation at 10,000 × *g* at 4 °C for 20 min, the supernatant was subjected to Triton X-114 phase-partitioning at 37 °C for 10 min. The detergent phase was resuspended with an equal volume of 50 mM Tris–HCl (pH 7.4) containing 150 mM NaCl. Solubilized membrane proteins in the detergent phase were precipitated with cold acetone and were resuspended in 400 μl of 50 mM Tris–HCl (pH 7.4). Following the addition of PIPLC (1 U), the suspension was incubated at 37 °C for 18 h. The suspension was resubjected to Triton X-114 phase-partitioning, and PIPLC-treated GPI-anchored proteins were precipitated with cold acetone from the aqueous phase. PIPLC-treated GPI-anchored proteins obtained from

50 mg of rat brain were separated by SDS-PAGE (12.5%) after carboxyamidomethylation [22].

2.3. Extraction and digestion of gel-separated proteins

The protein in gel band was extracted with 20 mM Tris–HCl containing 1% SDS by shaking vigorously overnight after breaking down the gel into small bits. The extract was filtered with Ultrafree-MC (0.22 μm, Millipore, Bedford, USA), and the protein was precipitated by adding cold acetone. The precipitate was digested with trypsin (1 μg) in 20 μl of 0.1 M Tris–HCl (pH8.0) at 37 °C for 16 h, or with Asp-N (0.4 μg) in 20 μl of 5 mM Tris–HCl (pH 7.5) at 37 °C overnight.

2.4. LC/MS^n

Proteolytic peptides were separated by a Magic C18 column (50 mm × 0.2 mm, 3 μm, Michrom BioResources, Auburn, CA, USA) with a Paradaim MS4 HPLC system (Michrom BioResources Inc., Auburn, CA, USA) consisting of pump A: 0.1% formic acid and 2% acetonitrile, and pump B: 0.1% formic acid and 90% acetonitrile. Separation was performed with a linear gradient of 5–65% of pump B in 40 min after 5% in 10 min of pump B at a flow rate 3 μl/min. Mass spectra were recorded by Finnigan LTQ (Thermo Electron, San Jose, CA, USA) with the sequential scan: a full mass scan (*m/z* 300–2000), a full mass scan with in-source CID (*m/z* 80–500, collision energy: 50 V), and data-dependent CID-MS^n for most intense ions at each scan with dynamic exclusion for 30 s. Scan time (*m/z* 300–2000) is approximately 0.1 s. The operating condition used for LC/ITMS was as follows: tube lens offset of 130 V, capillary voltage of 2.0 kV, capillary temperature of 200 °C.

2.5. Computer database search analysis

All product ions obtained by LC/ITMS were subjected to the computer database search analysis with the TurboSEQUEST search engine (Thermo Electron, San Jose, CA, USA). We used the NCBI database (rat, updated at February 2003) and following search parameters: a static modification of carboxyamidomethylation (57 Da) at Cys, a possible modification of GlcNAc (203 Da) at Asn, and trypsin used for digestion.

3. Results

3.1. Extraction of whole proteins from the gel

Rat brain PIPLC-treated GPI-anchored proteins were separated by SDS-PAGE (Fig. 1), and the most noticeable band at 20–25 kDa was cut off from the gel and crushed. The gel pieces were shaken vigorously in 1% SDS, and the extracted protein was precipitated with cold acetone to remove SDS.

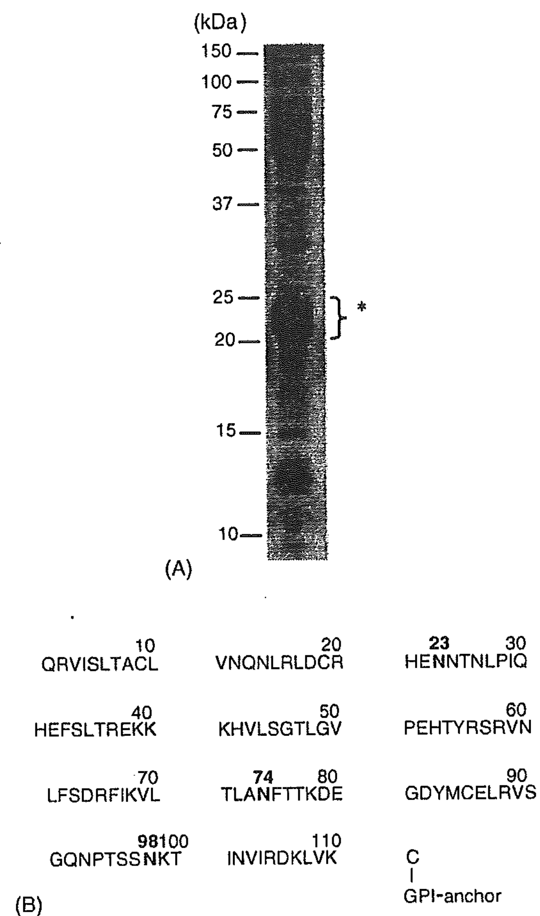

Fig. 1. (A) SDS-PAGE of PIPLC-treated GPI-anchored proteins from rat brain. (B) Amino acid sequence of rat Thy-1. *N*-Glycosylation sites are indicated by bold face. The protein at 20–25 kDa indicated by asterisk was subjected to the glycosylation analysis in this study.

We checked the recovery of the protein at 20–25 kDa by comparing the fluorescence intensity (Ex 633 nm/Em 670 nm) of the proteins at 20–25 kDa visualized by Coomassie staining before and after extraction. Approximately 55% of the protein at 20–25 kDa could be recovered from the gel (data not shown). The protein was digested with trypsin and subjected to the sequential scan consisting of full mass scans with and without in-source CID and data-dependent MS^n by LC/ITMS for protein identification and glycosylation analysis.

3.2. Database search analysis

Fig. 2(A) shows the peptide/glycopeptide map of the trypsin-digested protein at 20–25 kDa. First, all product ions generated by data-dependent MS^n were used for the database search analysis. Using search parameters described in Section 2.5, the protein was identified as Thy-1, a glycoprotein containing three *N*-glycosylation sites at Asn23, 74, and 98, and a GPI attachment site at Cys111. The search analysis also suggested the glycosylation at Asn74 and 98, with elution positions of 34 min (peak T6, Val69-Lys78) and 3.5 min (peak T1, Val89-Lys99), respectively (Fig. 2(A)). Although

Table 1
Glycosylation analysis of rat brain Thy-1

Glycosylation site	Carbohydrate composition[a]				Theoretical carbohydrate mass[b]	Trypsin					Asp-N				
	dHex	Hex	HexNAc	NeuAc		Observed m/z	Charge state	Peak number	Amino acid residue[c]	Theoretical m/z[b]	Observed m/z	Charge state	Peak number	Amino acid residue[c]	Theoretical m/z[b]
Asn23	0	5	2	0	1234.43	845.33	3	T3	H21-H31 (1315.63)	845.03	799.47	3	A3	E22-H31 (1178.57)	799.34
						937.27	3	T4	H21-F33 (1591.74)	937.06	1198.69	2	A3	E22-H31 (1178.57)	1198.50
						1405.81	2	T4	H21-F33 (1591.74)	1405.09	949.60	3	A3	N23-T36 (1626.80)	948.75
											1423.40	2	A3	N23-T36 (1626.80)	1422.62
	0	6	2	0	1396.49	899.49	3	T3	H21-H31 (1315.63)	899.04	853.54	3	A3	E22-H31 (1178.57)	853.36
						1348.35	2	T3	H21-H31 (1315.63)	1348.06	1279.66	2	A3	E22-H31 (1178.57)	1279.53
						942.16	3	T3	H21-E32 (1444.67)	942.06	1211.52	2	A5	E22-Q30 (1041.51)	1211.00
						991.37	3	T5	H21-F33 (1591.74)	991.08					
						1486.40	2	T5	H21-F33 (1591.74)	1486.12					
	0	3	5	0	1519.57						1044.43	3	A3	N23-T36 (1626.80)	1043.79
	0	7	2	0	1558.54	996.41	3	T3	H21-E32 (1444.67)	996.07	907.59	3	A3	E22-H31 (1626.80)	907.37
											1361.03	2	A3	E22-H31 (1178.57)	1360.56
	1	3	5	0	1665.62						1093.32	3	A3	N23-T36 (1626.80)	1092.48
	1	5	4	0	1786.65						1133.80	3	A3	N23-T36 (1626.80)	1132.82
	0	6	3	1	1890.66						1168.51	3	A4	N23-T36 (1626.80)	1167.49
	1	6	4	0	1948.70						1187.21	3	A3	N23-T36 (1626.80)	1186.84
Asn74	1	2	3	0	1405.52	1026.26	3	T6	V59-F75 (1996.12)	1026.18					
	0	5	2	0	1234.43	949.52	2	T2	A73-K78 (680.35)	949.39	995.71	3	A7	D64-K78 (1766.01)	995.15
						1162.72	2	T6	V69-K78 (1106.62)	1162.53					
	1	4	3	0	1421.52	1043.45	2	T2	A73-K78 (680.35)	1042.94					
	1	3	4	0	1462.54	1063.68	2	T2	A73-K78 (680.35)	1063.45					
						1276.61	2	T6	V69-K78 (1106.62)	1276.58					
	1	5	3	0	1583.57	1124.18	2	T2	A73-K78 (680.35)	1123.96					
						1337.64	2	T6	V69-K78 (1106.62)	1337.10					
	1	3	5	0	1665.62	1165.13	2	T2	A73-K78 (680.35)	1164.99	1272.15	2	A4	T71-K78 (894.48)	1272.05
						919.71	3	T6	V69-K78 (1106.62)	919.09	1139.79	3	A7	D64-K78 (1766.01)	1138.88
						1378.19	2	T6	V69-K78 (1106.62)	1378.12					
	2	5	3	0	1729.63	1197.53	2	T2	A73-K78 (680.35)	1196.99					
	2	4	4	0	1770.66	1217.67	2	T2	A73-K78 (680.35)	1217.51					
						1430.71	2	T6	V69-K78 (1106.62)	1430.64					
	1	5	4	0	1786.65	1226.38	2	T2	A73-K78 (680.35)	1225.50					
						960.01	3	T6	V69-K78 (1106.62)	959.43					
						1439.05	2	T6	V69-K78 (1106.62)	1438.64					
	1	4	5	0	1827.68	973.79	3	T6	V69-K78 (1106.62)	973.10					
	2	5	4	0	1932.71	1298.75	2	T2	A73-K78 (680.35)	1298.53	1228.18	3	A7	D64-K78 (1766.01)	1227.91
						1008.71	3	T6	V69-K78 (1106.62)	1008.11					
						1512.21	2	T6	V69-K78 (1106.62)	1511.67					
	1	6	4	0	1948.70	1306.81	2	T2	A73-K78 (680.35)	1306.53					
						1013.98	3	T6	V69-K78 (1106.62)	1013.45					
	0	4	5	1	1972.71						1241.91	3	A7	D64-K78 (1766.01)	1241.25
	2	4	5	0	1973.73	880.04	3	T2	A73-K78 (680.35)	879.70	1241.84	3	A7	D64-K78 (1766.01)	1241.59
						1319.24	2	T2	A73-K78 (680.35)	1319.04					
						1022.43	3	T6	V69-K78 (1106.62)	1021.79					
						1532.49	2	T6	V69-K78 (1106.62)	1532.49					